Received: 14 March 2025 | Revised: 21 July 2025 | Accepted: 22 July 2025

DOI: 10.1111/bph.70176

RESEARCH ARTICLE

In silico, in vitro and ex vivo characterization of cystic fibrosis transmembrane conductance regulator pathogenic variants localized in the fourth intracellular loop and their rescue by modulators

Emanuela Pesce[1] | Valeria Tomati[1] | Valeria Capurro[1] | Mariateresa Lena[2] | Cristina Pastorino[1] | Miro Astore[3] | Serdar Kuyucak[3] | Benoit Chevalier[4,5] | Elvira Sondo[1] | Federico Cresta[6] | Alice Dighero[1] | Vito Terlizzi[7] | Cristina Fevola[7] | Stefano Costa[8] | Maria Cristina Lucanto[8] | Valeria Daccò[9] | Laura Claut[9] | Francesca Ficili[10] | Benedetta Fabrizzi[11] | Renata Bocciardi[1,2] | Federico Zara[1,2] | Carlo Castellani[6] | Luis J. V. Galietta[12] | Shafagh A. Waters[13,14,15,16] | Alexandre Hinzpeter[4,5] | Nicoletta Pedemonte[1]

Correspondence
Nicoletta Pedemonte, UOC Genetica Medica, IRCCS Istituto Giannina Gaslini, Genoa, Italy.
Email: nicolettapedemonte@gaslini.org

Funding information
This work was supported by Fondazione per la Ricerca sulla Fibrosi Cistica grants FFC #9/2019 (with the contribution of 'Delegazione FFC di Genova con Gruppo di sostegno FFC di Savona Spotorno', 'Delegazione FFC Ricerca di Valle Scrivia Alessandria', 'Delegazione FFC Ricerca di Montescaglioso' and 'Delegazione FFC Ricerca di Ascoli Piceno') and FFC #10/2021 (with the contribution of 'Delegazione FFC Ricerca di Genova', 'Delegazione FCC Ricerca Altomilanese', 'Gruppo di sostegno FFC Ricerca di Campiglione Fenile' and 'Delegazione FFC Ricerca di Napoli'), by Ministero della Salute through Cinque per mille (5Xmille 2019 grant 5M-2019-23680413) and Ricerca Corrente and grants GR-2018–12367126 and PNRR-MR1-2023-12378412 and by Cystic Fibrosis Foundation grant PEDEMO20G0. M. A. is supported by the Simons Foundation.

Background and Purpose: Cystic fibrosis (CF) is due to loss-of-function variants of the CF transmembrane conductance regulator (CFTR) channel. The most effective treatment for people with CF carrying the F508del mutation is the triple combination of elexacaftor–tezacaftor–ivacaftor (ETI). ETI can correct the underlying defect(s) in other CFTR mutants. The use of disease-relevant predictive models such as patient-derived human nasal epithelial cells allow to investigate the response to CFTR modulators of specific genotypes, possibly supporting patients' access to treatment.

Experimental Approach: Using computational, biochemical and functional methodologies, a detailed analysis of selected variants in the intracellular loop 4 (ICL4) to understand their impact on CFTR structure and function.

Key Results: Mutations affecting L1065, R1066 and L1077 compromise structural stability of CFTR. Analyses of single variants expressed heterologously in immortalized bronchial cells showed that, upon ETI, rescued activity for both L1065P and R1066C was close to 50% of the wild-type CFTR activity. Biochemical studies of ICL4 variants expression pattern in CFBE41o-cells, following treatment for 24 h, demonstrate the appearance of the mature, fully glycosylated band, with no changes in the immature band. Finally, our study provides evidence in primary nasal cells from

Abbreviations: CF, cystic fibrosis; EMA, European Medicines Agency; ETI, elexacaftor–tezacaftor–ivacaftor; FDA, Food and Drug Administration; HNEC, human nasal epithelial cells; HS-YFP, halide-sensitive yellow fluorescent protein; ICL4, intracellular loop 4; YFP, yellow fluorescent protein.

For affiliations refer to page 15

a cohort of people with CF that L1065P and R1066C can be effectively rescued by ETI up to 25%–45% of the activity measured in non-CF epithelia.

Conclusion and Implications: Although the observed rescue for L1065P and R1066C was smaller than that of the F508del, it should fall in a range predicted, by various studies, to provide a clinical benefit.

KEYWORDS
CFTR modulators, chloride channel, correctors, personalized medicine, potentiators, predictive models, theratyping

1 | INTRODUCTION

Cystic fibrosis (CF) is the most prevalent and life-limiting genetic disorder, due to loss-of-function variants in the **CF transmembrane conductance regulator (CFTR) gene**, which encodes the **CFTR** chloride/bicarbonate channel. The CFTR protein is prominently expressed on the apical membrane of various cell types, particularly epithelial cells (Cutting, 2015). Although CF is a multi-organ disease, its morbidity and mortality remains mostly related to the respiratory symptoms. In the airways, CFTR dysfunction impairs chloride/bicarbonate secretion, leading to increased mucus viscosity and compromised mucociliary clearance, which in turn facilitates bacterial infections and chronic inflammation, ultimately causing airway obstruction and reduced respiratory function (Castellani & Assael, 2017).

Structurally, the CFTR anion channel consists of 1480 amino acids, organized into two membrane spanning domains (MSD1 and MSD2), each containing six transmembrane helices, two nucleotide binding domains (NBD1 and NBD2) and a regulatory (R) domain (Csanady et al., 2019; Meng et al., 2019). The amino-terminal region, which includes the 'lasso' domain, and the carboxy-terminal region of CFTR are cytosolic (Csanady et al., 2019; Meng et al., 2019). The gating of the CFTR pore, formed by the membrane spanning domains, is regulated by phosphorylation of the R domain by the **cAMP-dependent protein kinase A** and is further modulated by **ATP** binding and hydrolysis at the nucleotide binding domains (Csanady et al., 2019; Meng et al., 2019).

To date, more than 2100 CFTR variants have been identified, with 1085 classified as pathogenic (CF-causing) in the Clinical and Functional CFTR database (CFTR2; https://cftr2.org; accessed on 18 October 2024), while another 55 variants are annotated as variants of varying clinical consequence. These pathogenetic variants impair CFTR function through various mechanisms (De Boeck & Amaral, 2016). The most frequent CF-causing mutation, F508del, accounts for 70% of the pathogenetic alleles (Beaudet, 1992). Other variants are generally rare, ultra-rare or even private, that is, unique to a single individual or a very small group within a population (CFTR2; https://cftr2.org; accessed on 18 October 2024). The F508del-CFTR protein displays defective folding, leading to its retention in the endoplasmic reticulum and premature degradation through the ubiquitin-proteasome system, thus failing to traffic to the plasma membrane (Veit et al., 2016). Furthermore F508del-CFTR protein shows abnormal gating, responding inadequately to **cAMP** stimulus.

CFTR modulators, such as correctors and potentiators, are small molecules designed to rescue defective protein folding or channel gating, respectively (Lopes-Pacheco, 2019). Currently, the most effective treatment for people with CF carrying one or two copies of the F508del mutation is a combination therapy comprising two correctors, **elexacaftor** (ELX) and **tezacaftor** (TEZ), with the potentiator **ivacaftor** (IVA), referred to as ELX/TEZ/IVA or ETI (Bacalhau et al., 2023). Elexacaftor and tezacaftor exert additive effects, restoring F508del protein trafficking to the plasma membrane and hence chloride transport to ~60%–65% of wild-type CFTR levels (Capurro et al., 2021; Veit et al., 2020). Tezacaftor and its analogue **lumacaftor** (Van Goor et al., 2011) are classified as Type 1 correctors, binding to membrane spanning domain 1 (Fiedorczuk & Chen, 2022a), while elexacaftor is classified as a Type 3 corrector, binding to Helix 11 of membrane

What is already known?

- CFTR ICL4 variants are expressed only as immature, core-glycosylated forms, indicating improper processing.

What does this study add?

- Mutations affecting L1065, R1066 and L1077 compromise structural stability of CFTR.
- ETI rescues L1065P and R1066C up to 25%–45% of normal CFTR activity in nasal epithelia.

What is the clinical significance?

- The observed rescue falls in a range predicted to provide a clinical benefit.

spanning domain 2 and the 'lasso' domain (Fiedorczuk & Chen, 2022b). Interestingly, although initially developed for F508del, CFTR modulators can correct the underlying defect(s) in other CFTR mutants (Bear & Ratjen, 2023; Dreano et al., 2023).

Regulatory agencies differ in their approach to the approval of CFTR modulators. Until February 2025, the European Medicines Agency (EMA) granted approval for ETI exclusively for F508del mutation, based on robust clinical trial data demonstrating its efficacy. In contrast, the US Food and Drug Administration (FDA) not only approved ETI for F508del but also extended its approval to an additional 177 CFTR variants. This broader FDA approval was supported by *in vitro* data, demonstrating ETI efficacy to rescue various CFTR mutants expressed in the Fischer rat thyroid (FRT) heterologous expression system. Responsiveness to ETI was determined based on a cut-off value for rescued activity of at least 10% of wild-type CFTR activity (a press release can be found at: https://investors.vrtx.com/news-releases/news-release-details/vertex-announces-fda-approvals-trikaftar). Recently, the same approach was applied by the Cystic Fibrosis Foundation Therapeutics Laboratory to evaluate the responsiveness of 655 CFTR variants (Bihler et al., 2024).

An alternative option to assess drug efficacy involve the use of standardized predictive models based on patient-derived cells (Berkers et al., 2019; Pedemonte, 2022). Multiple studies have established a correlation between data from these models and the clinical outcomes for people with CF with different variants (Allan et al., 2022; Allan et al., 2023; Brewington et al., 2018; Dreano et al., 2023; Graeber et al., 2023; Sadras et al., 2023; Sondo et al., 2022; Tomati et al., 2023). Consequently, these predictive models could offer a viable means to collect efficacy data for variants that lack approved therapies but are potentially responsive.

Among the variants still lacking approved therapies there are L1065P and R1066C, located in the C-terminal intracellular loop (ICL4; residues 1035–1102) of the CFTR chloride channel. Previous studies have investigated the impact of several missense variants within ICL4 on CFTR protein maturation and channel activity, revealing that 12 out of 18 ICL4 variants were expressed only as immature, core-glycosylated forms, indicating improper processing in HEK-293 cells (Seibert et al., 1996). Some of these variants, such as R1066H or L1077P are already deemed eligible for ETI (elexacaftor–tezacaftor–ivacaftor) therapy based on data from Fischer rat thyroid studies by the FDA, while others, such as L1065P and R1066C, remain poorly characterized.

The CFTR2 database (accessed on 23 October 2024) records 63 alleles bearing the L1065P variants among the 211,106 identified variants in 122,935 people with CF, with a notable prevalence of 1.3% in Southern Italy (Castaldo et al., 1999). Similarly, the R1066C variant, reported in 532 alleles, is particularly common among people with CF from Portugal and Spain (Estivill et al., 1997). In this study, we present a comprehensive characterization of the L1065P and R1066C mutations, comparing them with other ICL4 variants using computational studies as well as functional and biochemical analyses in primary and immortalized airway cell models.

2 | METHODS

2.1 | Patients under study

The following patients (donor IDs and corresponding genotypes) were included in this study: FI114 (L1065P/Dele2), FI054 (L1065P/G542X), FI039 (L1065P/N1303K), ME372 (L1065P/N1303K), FI140 (L1065P/R117C), GE202 (R1066H/Dele2ins182), ME086 (R1066H/N1303K), GE166 (R1066H/1717-1G>A), MI279 (R1066H/G542X), GE385 (R1066H/G542X), ME122 (R1066C/R1066C), GE006 (R1066C/N1303K), GE001 (R1066C/G542X), GE200 (L1077P/Dele2,3), ME106 (L1077P/G542X), ME096 (L1077P/N1303K), ME085 (L1077P/R1066C), ME107 (L1077P/R1158X), ME298 (L1077P/E585X) and GE348 (L1077P/1717-1G>A). Nine healthy subjects (donor IDs: Ctr010, Ctr069, Ctr147, Ctr153, Ctr178, Ctr191, Ctr192, Ctr323 and Ctr362), four subjects homozygous for F508del (donor IDs: AN232, TT003, TT005 and AN235) and one compound heterozygous (AN238, F508del/2183AA>G) were enrolled as further controls.

2.2 | Molecular dynamics

The CFTR protein model used for molecular dynamics simulations was based on the ATP-bound human CFTR cryogenic electron microscopy (cryo-EM) structure (PDB ID: 6MSM) (Zhang et al., 2018). The construction of the CFTR protein system, included modelling part of the R domain, was described previously (Wong et al., 2022). In brief, the CFTR was embedded in a simplified cell membrane model containing pure 1-palmitoyl-2-oleoyl-sn-glycero-3-phosphocholine (POPC) lipids then solvated with 150-mM NaCl on both the cytoplasmic and periplasmic sides.

In this study, the software Gromacs v2021.1 (RRID:SCR_014565) (Van Der Spoel et al., 2005) was used for all MD simulations. Molecular mechanics parameters were supplied via the CHARMM36m (Huang et al., 2017) force field with the following modifications for faster simulation performance: virtual site topologies (Feenstra et al., 1999) for all molecules while using MkVsite (Larsson et al., 2020) to generate topologies for the ATP molecule, as well as parameter adjustments specific to lipids (Olesen et al., 2018). The initial positions of all molecules were equilibrated for production runs in two phases: first via energy minimisation using a steepest descent algorithm, then followed by a 6-ns simulation where position-restraints on all non-hydrogen atoms were imposed and then gradually relaxed.

A series of 2-μs production MD simulations were carried out, with three replicates each of WT, L1065P, R1066C and L1077P-CFTR. To decrease computational expense, elevated temperatures of 350 K (77°C) were used to accelerate conformational transitions, in addition to simulations at physiological temperatures of 310 K (37 °C). The use of elevated temperatures to study defects in mutant CFTR was validated previously (Wong et al., 2022). Scripts may be found at https://github.com/miro-astore/mdanalysis_scripts and https://github.com/miro-astore/gromacs_scripts.

2.3 | Vectors and CFTR modulators

Vectors encoding WT-, L1065P-, L1065R-, R1066C-, R1066H-, L1077P- and F508del-CFTR variants were purchased from VectorBuilder (vector IDs available upon request; Neu-Isenburg, Germany).

The CFTR modulator elexacaftor was purchased from MedChemExpress (catalogue ID: HY-111772; Monmouth Junction, NJ, USA). Ivacaftor, lumacaftor and tezacaftor were obtained from TargetMol (catalogue ID: T2588, T2595 and T2263, respectively; Wellesley Hills, MA, USA). The final working concentrations used for the indicated CFTR modulators were as follows:- elexacaftor, 3 μM; lumacaftor, 3 μM; tezacaftor, 10 μM; ivacaftor, 0.1 μM (when applied acutely during short-circuit current measurements) or 1 μM (for the YFP assay) or 5 μM (for biochemical analysis, 24-h treatments). CFTR modulators were dissolved in DMSO.

2.4 | Cell culture

Isolation, culture and differentiation of primary human nasal epithelial cells (HNEC) were performed as previously detailed (Sondo et al., 2022; Terlizzi et al., 2023; Tomati et al., 2023). In brief, HNEC were obtained through a nasal brushing. Cells were subsequently cultured and expanded in PneumaCult Ex-Plus medium (StemCell Technologies, Vancouver, BC, Canada), supplemented with ROCK and **SMAD** inhibitors (DMH-1, A-83-01 and **Y27632** compounds). During the **first** days of culture, the medium was also supplemented with a mixture of different antibiotics (**colistin**, **piperacillin** and **tazobactam**) to eradicate any bacterial contamination. Nasal cells were seeded at high density (500,000 cells·cm^{-2}) on porous membranes (Snapwell inserts, Code 3801, Corning Life Sciences, Corning, NY, USA) to obtain differentiated epithelia. Twenty-four hours after seeding, the medium was removed from both sides of the porous membrane and replaced with Pneumacult ALI medium (StemCell Technologies, Vancouver, BC, Canada) on the basolateral side only. Epithelia differentiation (up to 16–18 days) was performed in air-liquid interface (ALI) condition.

Nasal epithelia with transepithelial resistance (Rt) ranging between 400 and 600 Ω cm^2 (thus forming electrically tight epithelia; Noel et al., 2021; Tomati et al., 2023) were used for the short-circuit current analysis.

CFBE41o-cells stably expressing the halide-sensitive yellow fluorescent protein (HS-YFP) were grown in MEM medium (Euroclone, Milan, Italy) supplemented with 10% FBS, 2-mM L-glutamine, 100-U/ml penicillin and 100-μg/ml streptomycin. Cells were plated at 80% confluence on clear-bottom 96-well black microplates (Corning Life Sciences, Corning, NY, USA) or 6-well plates (Euroclone, Milan, Italy) to perform the functional HS-YFP-based assay or for CFTR biochemical analysis, respectively.

2.5 | Short-circuit current recordings

Transepithelial ion transport analysis was performed using established methodologies (Sondo et al., 2022; Terlizzi et al., 2023; Tomati et al., 2023; Tomati et al., 2024). In brief, nasal epithelia differentiated on snapwell inserts were mounted in a vertical diffusion chamber resembling a Ussing chamber with internal fluid circulation. Apical and basolateral hemichambers were filled with 5 ml of a solution containing (in mM) 126 NaCl, 0.38 KH_2PO_4, 2.13 K_2HPO_4, 1 $MgSO_4$, 1 $CaCl_2$, 24 $NaHCO_3$ and 10 glucose. Both sides were continuously bubbled with a gas mixture containing 5% CO_2–95% air. Measurements were performed at 37°C. The transepithelial voltage was short-circuited with a voltage-clamp (DVC-1000, World Precision Instruments, Sarasota, FL, USA; VCC MC8 Physiologic Instruments, Reno, NV, USA) connected to the apical and basolateral chambers via Ag/AgCl electrodes and agar bridges (1-M KCl in 2% agar). Before the experiment, the transepithelial voltage was clamped at 0 mV after correcting voltage offsets and fluid resistance compensation. The short-circuit current was recorded by analogical to digital conversion on a personal computer.

2.6 | Transient transfection of CFBE41o-cell line

For the YFP assay, CFBE41o-cells stably expressing the HS-YFP (Galietta et al., 2001) were reverse-transfected onto 96-well plates with 0.2 μg per well of the indicated mutant CFTR vectors (see 'Chemicals and Vectors' in Section 2). To analyse CFTR expression by Western blotting, CFBE41o-cells were reverse-transfected onto 6-well plates with 2 μg of the indicated mutant CFTR vectors. Cells were transfected in Opti-MEM Reduced Serum Medium (ThermoFisher Scientific, Waltham, MA, USA) using Lipofectamine 2000 (ThermoFisher Scientific, Waltham, MA, USA) as transfection agent. After 6 h, Opti-MEM medium was replaced with MEM without antibiotics. Twenty-four hours after transfection and plating, cells were treated with correctors or vehicle alone (DMSO) at the indicated concentrations and incubated at 37°C for an additional 24 h, prior to proceeding with the functional or biochemical assays.

2.7 | YFP-based assay for CFTR activity on CFBE41o-cells

The HS-YFP microfluorimetric assay was used to evaluate CFTR activity on HEK293 and CFBE41o-cells as previously described (Sondo et al., 2022; Terlizzi et al., 2023; Tomati et al., 2023). In brief, CFBE41o-cells were washed with PBS (containing, in mM, 137 NaCl, 2.7 KCl, 8.1 Na_2HPO_4, 1.5 KH_2PO_4, 1 $CaCl_2$ and 0.5 $MgCl_2$) and then incubated with 60 μl per well of PBS containing forskolin (20 μM) and ivacaftor (1 μM), for 25 min at 37°C to maximally stimulate the CFTR channel. Cells were then transferred to a microplate reader (FluoStar Galaxy or Fluostar Optima; BMG Labtech, Offenburg, Germany), equipped with high-quality filters for YFP (excitation HQ500/20X: 500 ± 10 nm, emission HQ535/30 M: 535 ± 15 nm; Chroma Technology, Bellows Falls, VT, USA). During each assay the YFP fluorescence was recorded continuously for 14 s, with 2 s before and 12 s after

injection of 165 µl of an iodide-containing solution (PBS in which Cl^- was replaced by I^-; final I^- concentration 100 mM). After subtracting the background, fluorescence data were normalized to the initial value. The I^- influx rate was determined by fitting the final 11 s of the data with an exponential function to extrapolate the initial slope (dF/dt).

2.8 | Transient transfection of HEK-293 cells and YFP-based assay for CFTR activity

HEK-293 cells were seeded in 12-well plates and co-transfected with 300 ng of halide-sensitive yellow fluorescent protein YFP-H148Q/I152L (Galietta et al., 2001) and 300 ng of mutant CFTR plasmids using Lipofectamine 3,000 (Thermo Fisher Scientific, Illkirch-Graffenstaden, France). The day after transfection, cells were transferred to poly-L-lysinecoated 96 well black/clear bottom microplates (Greiner-BioOne, Les Ulis, France). The next day, cells were incubated with the elexacaftor/tezacaftor (3 µM/10 µM) or DMSO (Sigma-Aldrich, Saint-Quentin-Fallavier, France) solvent control for 24 h. After treatment, plates were washed with PBS and each well incubated 30 min with 100 µl of PBS containing 8-(4-chlorophenylthio)-adenosine 3′,5′-cyclic monophosphate (CPT-cAMP, 100 µM) and 3-Isobutyl-1-methylxanthine (IBMX, 100 µM) with and without potentiator ivacaftor (1 µM). Plates were then transferred to a ClarioStar plate-reader (BMG Labtech, Ortenberg, Germany) equipped with an injector enabling continuous recording of fluorescence (YFP filters) during injection. After 3 s, 200 µl of PBS-NaI (PBS solution where NaCl is replaced with NaI) were injected (final NaI concentration of 91 mM) and fluorescence measured for another 30 s. Signal decay was fitted to an exponential function to derive the maximal slope corresponding to initial influx into the cells. Maximal slopes were converted to rates of change in intracellular I-concentration (in mM/s).

2.9 | Analysis of the CFTR expression pattern by western blotting

All immuno-related procedures used comply with the recommendations made by the *British Journal of Pharmacology* (Alexander et al., 2018).

Primary nasal epithelia lysates were generated following the previously described protocol (Sondo et al., 2022; Tomati et al., 2023). Briefly, mucus excess on the apical side of HNEC differentiated epithelia (ALI conditions for 16–18 days) was removed by washing with warm HBSS (137.93-mM NaCl, 5.33-mM KCl, 0.338-mM Na_2HPO_4, 0.441-mM KH_2PO_4, 0.406-mM $MgSO_4$, 1.261-mM $CaCl_2$, 0.492-mM MgCl2 and 5.555-mM glucose) containing 0.4% sodium bicarbonate for 3 h at 37°C. After washing twice with warm complete D-PBS, the apical side of the filters was dried. Basolateral culture medium (Pneumacult ALI; StemCell Technologies, Vancouver, BC, Canada) was changed and epithelia were treated with indicated correctors or vehicle (DMSO) for 24 h at 37°C. The following day, the newly produced mucus was removed by washing the apical side of epithelia with warm HBSS 0.4% sodium bicarbonate at 37°C for 30 min and then with warm complete D-PBS. Epithelia were then lysed on ice by applying 125 µl/filter of ice-cold RIPA buffer (50-mM Tris–HCl pH 7.4, 150-mM NaCl, 1% Triton X-100, 0.5% sodium deoxycholate and 0.1% SDS) plus proteases inhibitors (Merck KGaA, Darmstadt, Germany). Cell layers were scraped, collected in a tube and left on ice for 15 min. Lysate viscosity was reduced by applying needle syringe passages (5 × 22 G followed by 5 × 27 G). Lysates were then cleared by centrifugation (15,000 × *g* for 20 min at 4°C). After centrifugation, the supernatant was transferred to a new tube and stored at −80°C for subsequent analysis.

Cell lysates from CFBE41o-cells were generated and then processed as follows. After transfection (see Section 2.6) and treatment with CFTR modulators, CFBE41o-cells were grown to confluence. The day of cell lysis, cells were washed with ice-cold D-PBS without Ca^{2+}/Mg^{2+} and then lysed in RIPA buffer supplemented with a complete protease inhibitor cocktail (Merck KGaA, Darmstadt, Germany). Lysates were separated by centrifugation at 15,000 × *g* at 4°C for 10 min. The supernatant was transferred to a new tube and stored at −80°C for subsequent analysis.

Supernatant protein concentration was calculated using a BCA assay (ThermoFisher Scientific, Waltham, MA, USA) following the manufacturer instructions. Total cell lysates (25 µg for CFBE41o-samples, 60 µg for HNEC samples) were separated onto gradient 4%–15% Criterion TGX Precast gels (Bio-rad Laboratories Inc., Hercules, CA, USA), transferred to a nitrocellulose membrane using the Trans-Blot Turbo system (Bio-rad Laboratories Inc., Hercules, CA, USA) and analysed by western blotting. The following primary antibodies were used: mouse monoclonal anti-CFTR (ab596, IgG_{2b}, RRID:AB_2923486; provided by Martina Gentzsch, University of North Carolina at Chapel Hill and Cystic Fibrosis Foundation Therapeutics) and mouse monoclonal anti-GAPDH (sc-32233, $IgG1_k$, RRID:AB_627679; Santa Cruz Biotechnology, Inc.). Horseradish peroxidase (HRP)-conjugated anti-mouse IgG (ab97023, RRID:AB_10679675; Abcam) was used as secondary antibody. Antibodies were diluted in Tris Buffer Saline (50-mM Tris–HCl pH 7.4, 150-mM NaCl) 0.1% Tween-20 (TBST) with 5% nonfat dry milk (Merck KGaA, Darmstadt, Germany): Mouse monoclonal anti-CFTR ab596 was used at a 1:5000 dilution for CFBE41o- and at a 1:1000 dilution for HNEC western blots; mouse monoclonal anti-GAPDH was used at a 1:10,000 dilution; HRP-conjugated anti-mouse IgG was used at a 1:10,000 dilution for CFTR imaging and at a 1:20,000 dilution for GAPDH visualization. Immunoblots were visualized by chemiluminescence using the SuperSignalWest DURA Substrate (ThermoFisher Scientific, Waltham, MA, USA). Images of HNEC immunoblots were acquired with Molecular Imager ChemiDoc MP System and analysed with Image Lab software (Bio-rad Laboratories Inc., Hercules, CA, USA) following manufacturer's instructions. For each lane CFTR protein profile was normalized against the corresponding GAPDH protein profile. Images of CFBE41o-immunoblots were acquired with

Molecular Imager ChemiDoc MP System (Bio-rad Laboratories Inc., Hercules, CA, USA) and analysed with ImageJ software (RRID:SCR_003070, National Institutes of Health, Bethesda); protein bands were analysed as region-of-interest (ROI), normalized against the GAPDH loading control.

2.10 | Cell surface quantification

CFTR cell surface was measured using hIBIT complementation (N2420, Promega, Charbonnières-les-Bains, France). This assay is based on the reconstitution of the nanoluciferase activity which is split in two parts: an 11 amino acid peptide (smBIT) and a large subunit (lgBIT).

HEK-293 cells plated in 12-well plates were transfected using Lipofectamine 3000 (#L3000-015, Thermo Fisher Scientific, Illkirch-Graffenstaden, France) with a total of 0.6 µg of plasmid. Transfected HEK-293 cells were plated in white 96-well plates and 24 h after transfection cells were washed and incubated with a recombinant lgBIT and furimazin substrate to measure cell surface CFTR. Cells were then permeabilized using Triton ×100 inducing the diffusion of the LgBIT inside the cells and enabling to quantify the total amount of CFTR. Quantification were performed quantifying the Surface-CFTR/Total-CFTR ratio normalized to the WT ratio. Detection of the produced luminescent is performed on a Mitras plate reader (Berthold, Thoiry, France).

2.11 | Statistics

The data and statistical analysis comply with the recommendations on experimental design and analysis in pharmacology (Curtis et al., 2025). The Kolmogorov–Smirnov test was applied to assess the assumption of normality of data. For normally distributed quantitative variables, when comparing more than two groups, a parametric analysis of variance (ANOVA) followed by a post-hoc test was used to avoid 'multiple comparisons error'. Post hoc tests were conducted only if F in ANOVA achieved $P < 0.05$. As post hoc test we applied the Dunnet test to assess statistical significance of

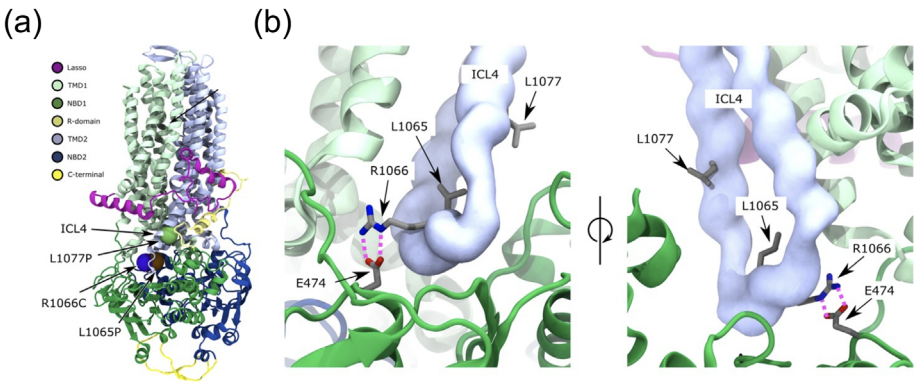

FIGURE 1 The architecture of cystic fibrosis transmembrane conductance regulator (CFTR) with the centrality of intracellular loop 4 (ICL4) highlighted. (a) CFTR has two transmembrane domains. ICL4 is situated in the middle of TMD2 where it makes direct contact with nucleotide binding domain (NBD) 1. (b) ICL4 is secured by a salt bridge between R1066 (within ICL4) and E474 (on NBD1) as well as several hydrophobic amino acids.

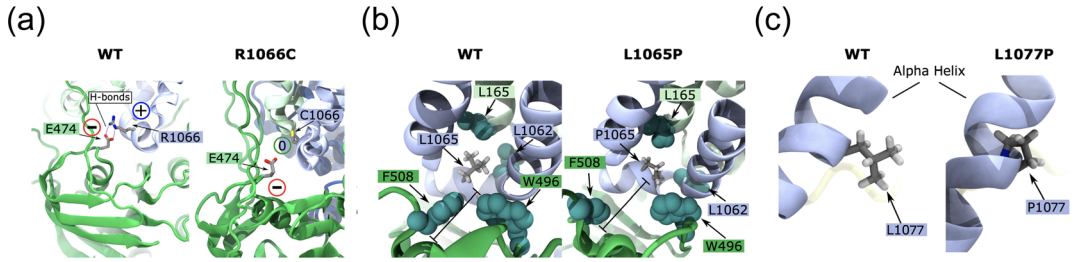

FIGURE 2 Structural impact of mutations within the intracellular loop 4 (ICL4) of cystic fibrosis transmembrane conductance regulator (CFTR). (a) Disruption of the salt bridge between nucleotide binding domain 1 (NBD1) and ICL4 caused by the R1066C mutation. In WT CFTR, R1066 forms a stable salt bridge with E474, supporting domain interactions. The R1066C mutation results in the loss of a positive charge, leading to the disruption of this critical salt bridge and compromising protein stability. (b) Structural dynamics of the L1065P mutation in ICL4. In wild-type (WT) CFTR, L1065 is positioned on an alpha helix, forming a hydrophobic pocket through interactions with residues F508, L165 and W496. These interactions contribute to proper protein folding and stability. The mutation to proline (L1065P) reduces these hydrophobic contacts and disrupts the hydrogen bonding required for alpha helix formation, leading to decreased stability of ICL4. (c) The effect of the L1077P mutation, which introduces a proline into an alpha helix within ICL4. The presence of proline distorts the helical structure, reducing the stability of the intracellular loop and potentially impacting CFTR function.

the effect of drug treatments, the Tukey test in the case of combinations of drugs and Bonferroni when comparing selected pairs of treatment. Normally distributed data are expressed as the mean ± SD and significances are two-sided. Differences were considered statistically significant when $P < 0.05$. Statistical analysis was performed only when the number of biological replicates was ≥ 5 per experimental condition.

2.12 | Materials

The following compounds were obtained from Selleck Chemicals GmbH (Planegg, Germany): - elexacaftor, lumacaftor, tezacaftor and ivacaftor, while 8-(4-chlorophenylthio)-adenosine 3′,5′-cyclic monophosphate (CPT-cAMP), 3-Isobutyl-1-methylxanthine (IBMX), poly-L-lysine, DMSO, triton-100 (#T9284) from Sigma-Aldrich

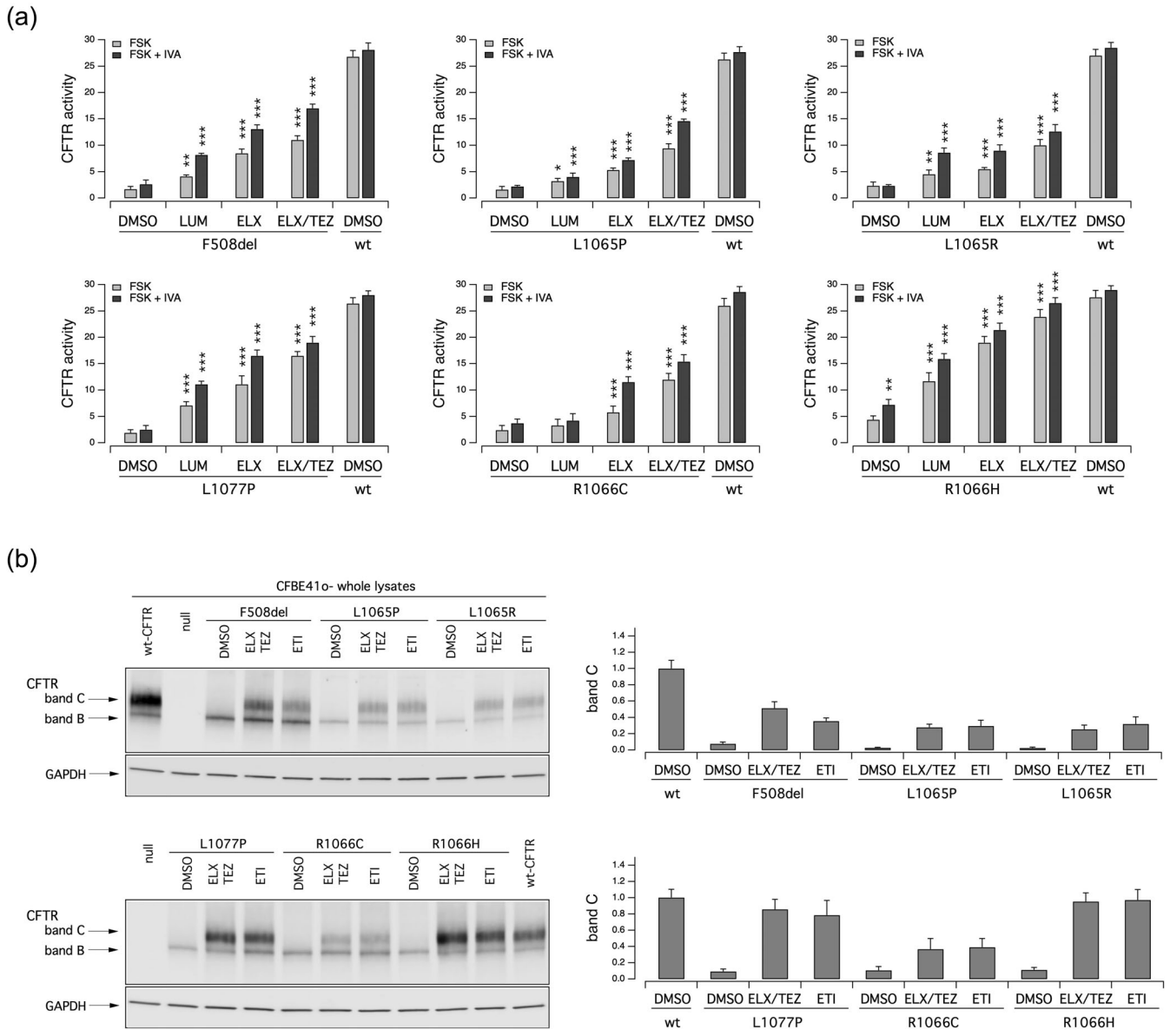

FIGURE 3 Functional and biochemical evaluation of the effect of cystic fibrosis transmembrane conductance regulator (CFTR) modulators on intracellular loop 4 (ICL4) variants in immortalized bronchial cells. (a) The bar graph shows the activity (mean ± SD; n = 6) of the indicated CFTR variants transiently expressed in CFBE41o-cells stably expressing the halide-sensitive yellow fluorescent protein (HS-YFP). CFTR activity was determined as a function of the YFP quenching rate following iodide influx elicited by forskolin (FSK; 20 μM; light grey bars) or forskolin + ivacaftor (IVA) (1 μM; dark grey bars) in cells treated for 24 h with DMSO (vehicle), or lumacaftor (LUM; 3 μM), or elexacaftor (ELX; 3 μM) or ELX/tezacaftor (TEZ) (3 μM/10 μM). Data from cells transiently expressing F508del- and wt-CFTR are also shown for comparison. Asterisks indicate statistical significance of treatments: *$P < 0.05$; **$P < 0.01$; *** $P < 0.001$ versus DMSO/FSK condition. (b) Biochemical analysis of ICL4 variants expression pattern in CFBE41o-cells. The representative western blot image shows CFTR electrophoretic mobility in cell lysates following treatment for 24 h, prior to lysis, with the indicated modulators. Lysates from cells expressing wt- and F508del-CFTR are also shown for comparison, while lysates of parental cells have been included as control for antibody specificity. The bar graphs show CFTR band C densitometry (mean ± SD; n = 3) of the western blot experiments.

(Saint-Quentin-Fallavier, France). Further FBS, glutamine, penicillin and streptomycin were obtained from Euroclone (Milan, Italy). Colistin, piperacillin, tazobactam, ROCK and SMAD inhibitors (DMH-1, A-83-01 and Y-27632), amiloride, apigenin, CFTR inhibitor-172, and foskolin were obtained from TargetMol (Linz, Austria).

Details of other materials and suppliers are provided in the specific sections.

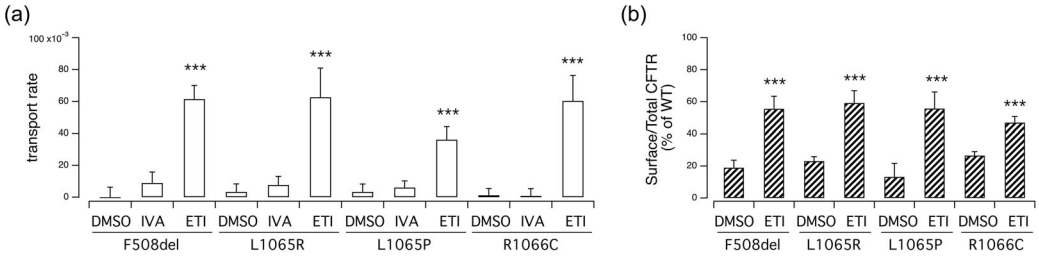

FIGURE 4 Analysis of the effect of cystic fibrosis transmembrane conductance regulator (CFTR) modulators on function and cell surface expression of intracellular loop 4 (ICL4) variants on HEK293 cells. (a) The bar graph shows the transport rate (mean ± SD; n = 6–8) of the indicated CFTR variants transiently expressed in HEK293 cells. The transport rate was determined as a function of the YFP quenching rate following iodide influx elicited by CPT-cAMP (100 μM) and IBMX (100 μM) without or with ivacaftor (1 μM) in cells treated for 24 h with DMSO (vehicle), or elexacaftor (ELX)/ tezacaftor (TEZ) (3 μM/10 μM). Data from cells transiently expressing F508del- and wt-CFTR are also shown for comparison. (b) Biochemical analysis of ICL4 variants expression on the cell surface in HEK293 cells. The bar graphs show the quantification of the surface-CFTR/Total-CFTR ratio (mean ± SD; n = 6–10) normalized to the WT ratio, determined by means of the hIBIT complementation experiments. Asterisks indicate statistical significance of treatments: $^{***}P < 0.001$ versus DMSO.

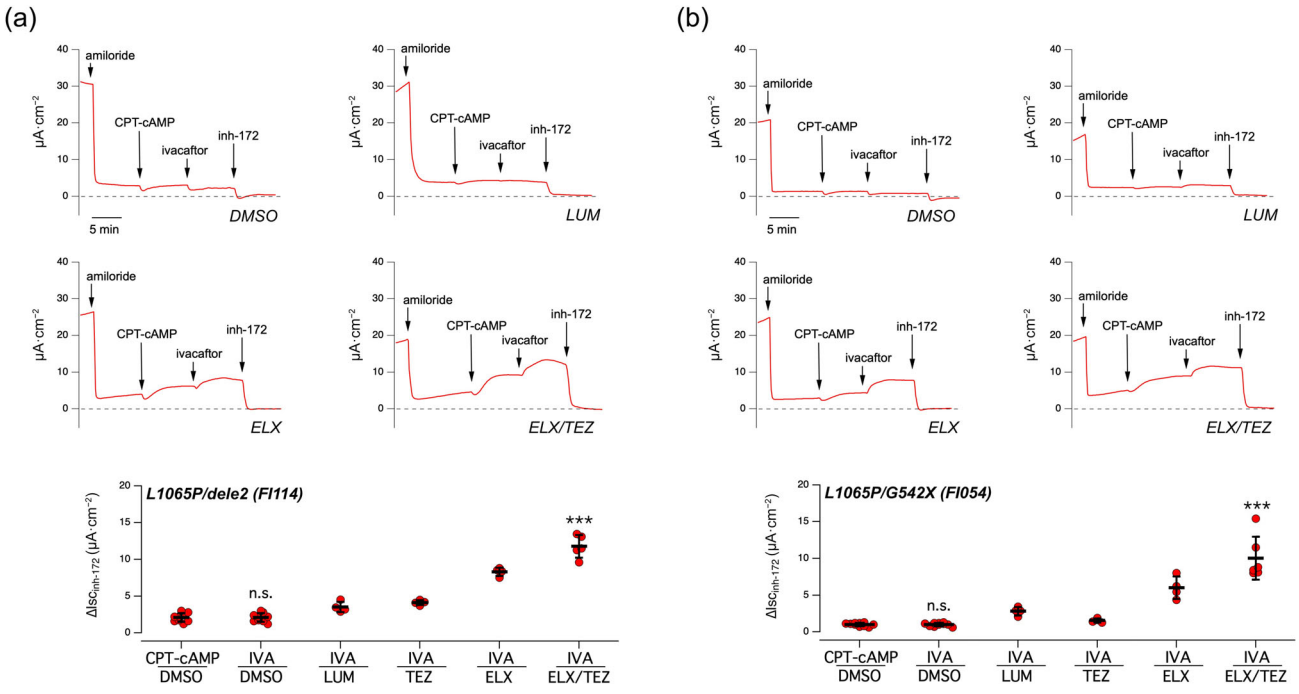

FIGURE 5 Functional evaluation of cystic fibrosis transmembrane conductance regulator (CFTR) activity and rescue by corrector treatment on nasal epithelia derived from L1065P/MF people with CF (pwCF). Epithelia were treated for 24 h with vehicle (DMSO), or tezacaftor (TEZ, 10 μM), or lumacaftor (LUM, 3 μM), or elexacaftor (ELX, 3 μM), or ELX/TEZ (3 μM/10 μM) prior to the assay. (a) Representative traces and scatter dot plot summarizing CFTR activity and the effect of drug treatments on L1065P/dele2 nasal epithelial cells (derived from donor ID: FI114; n = 4–9) measured with the short-circuit current technique. During the recordings, the epithelia were sequentially treated (as indicated by downward arrows) with amiloride (10 μM; added on the apical side), CPT-cAMP (100 μM; added on both apical and basolateral sides), ivacaftor (0.1 μM; apical side) and the CFTR inhibitor-172 (inh-172; 20 μM; apical side). The dashed line indicates zero current level. (b) Representative traces and scatter dot plot summarizing CFTR activity and the effect of drug treatments on L1065P/G542X nasal epithelial cells (donor ID: FI054; n = 4–9) measured with the short-circuit current technique. During the recordings, the epithelia were sequentially treated as detailed in (a). Symbols indicate statistical significance of treatments: n.s., not significant; $^{***}P < 0.001$ versus DMSO/CPT-cAMP condition. Statistical analysis was performed only for those experimental conditions having n ≥ 5.

2.13 | Nomenclature of targets and ligands

Key protein targets and ligands in this article are hyperlinked to corresponding entries in the IUPHAR/BPS Guide to PHARMACOLOGY http://www.guidetopharmacology.org and are permanently archived in the Concise Guide to PHARMACOLOGY 2023/24 (Alexander, Fabbro, et al., 2023; Alexander, Mathie, et al., 2023).

3 | RESULTS

3.1 | Mutations in the ICL4 loop of CFTR disrupt structural stability through altered hydrophobic interactions, salt bridge disruption and helical destabilization.

The ICL4 loop (P1050 to K1090) of CFTR is positioned in the middle of TMD2 and directly contacts nucleotide binding domain 1, playing a crucial role in the conformational stability of the protein (Figure 1a). This study focuses on three mutations within ICL4:- L1065P, R1066C and L1077P. These mutations occur at the interface between nucleotide binding domain 1 and ICL4, directly anchoring the intracellular loop against the nucleotide binding domain which implicates them directly in pathogenesis of CFTR folding and function (Figure 1b).

Molecular dynamics simulations of these mutations show that each mutation produces changes to CFTR structure. The R1066C mutation involves the substitution of a positive arginine (R) with a neutral cysteine (C), resulting in the loss of a critical positive charge at this position (Figure 2a). In WT-CFTR, R1066 forms a stable salt bridge with E474, facilitating interactions between nucleotide binding domain 1 and ICL4 (Figure 2a). The mutation to cysteine disrupts this salt bridge, which is essential for maintaining the protein's stability, leading to a significant loss of structural integrity at the interface between ICL4 and NBD1 (Figure 2a). The L1065P mutation, where leucine (L) is substituted with proline (P), disrupts the formation of a hydrophobic pocket that typically supports proper folding (Figure 2b). In WT-CFTR, L1065 forms hydrophobic interactions with residues such as F508, L165 and W496, which stabilize the protein (Figure 2b). The mutation to proline results in fewer hydrophobic contacts and eliminates the supporting hydrogen bond required for alpha helix stability, leading to a localized structural disruption within ICL4 (Figure 2b). The L1077P mutation introduces a proline residue into an alpha helix, distorting the helical structure and reducing the stability of the intracellular loop (Figure 2c). The presence of proline in a helix

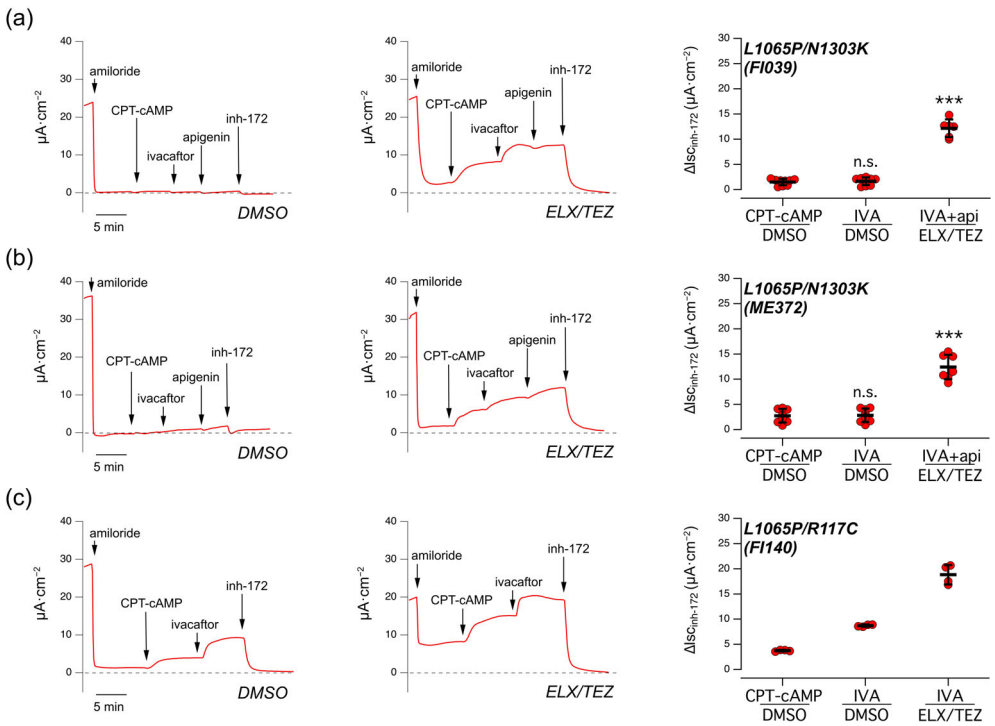

FIGURE 6 Functional evaluation of cystic fibrosis transmembrane conductance regulator (CFTR) activity and rescue by corrector treatment on nasal epithelia derived from people with CF (pwCF) bearing the L1065P in trans with another responsive variant. Epithelia were treated for 24 h with vehicle (DMSO), or elexacaftor (ELX)/tezacaftor (TEZ) (3 μM/10 μM) prior to the assay. (a,b) Representative traces and scatter dot plots summarizing CFTR activity and the effect of drug treatments on L1065P/N1303K nasal epithelial cells derived from donor IDs: FI039 (n = 6–9; a) and ME372 (n = 7–8; b) measured with the short-circuit current technique. (c) Representative traces and scatter dot plot summarizing CFTR activity and the effect of drug treatments on L1065P/R117C nasal epithelial cells (derived from donor ID: FI140; n = 4) measured with the short-circuit current technique. Symbols indicate statistical significance of treatments: n.s., not significant; $^{***}P < 0.001$ versus DMSO/CPT-cAMP condition. Statistical analysis was performed only for those experimental conditions having n ≥ 5.

is known to weaken the integrity of the helix and hence the overall folding stability of CFTR (Figure 2c) (Horovitz et al., 1992).

These *in silico* findings demonstrate that mutations affecting R1066, L1065 and L1077 result in disruptions of salt bridges, hydrophobic interactions and helical integrity, respectively, leading to compromised structural stability of ICL4 and CFTR as a whole. Overall, these structural defects provide insight into how mutations within ICL4 contribute to CFTR dysfunction, implicating their role in the pathology of cystic fibrosis.

3.2 | ICL4 variants display negligible activity due to defective protein maturation but can be rescued by elexacaftor–tezacaftor–ivacaftor (ETI) in heterologous expression systems

To characterize the functional defect of L1065P, CFBE41o-bronchial cells were transfected with the plasmids coding for L1065P and, for comparison, for L1065R and other ICL4 variants (R1066H, R1066C and L1077P) with known folding/activity defect (Seibert et al., 1996). Then, the cells were treated for 24 h with vehicle (DMSO) or with lumacaftor (3 μM), elexacaftor (3 μM) or elexacaftor/tezacaftor (3 μM/10 μM) (Figure 3a). As further control, we also included wild type and F508del CFTR (Figure 3a). Functional evaluation of CFTR was done by means of the HS-YFP-based assay (Pedemonte et al., 2011) which estimates CFTR activity as a function of the fluorescence quenching elicited by CFTR-mediated I^- influx. At the time of the assay, cells were acutely stimulated with a cAMP agonist (resembling the physiological stimulation) alone or in the presence of ivacaftor (1 μM). Figure 3a shows the results obtained for the different variants of CFTR. As expected, F508del-CFTR displayed negligible ivacaftor-stimulated activity that was increased upon chronic treatment with single correctors (with elexacaftor more effective than lumacaftor) and even further improved by co-treatment with the elexacaftor/tezacaftor. The five ICL4 variants displayed an activity profile similar to that of F508del (Figure 3a). The two ETI-eligible variants, R1066H and L1077P, showed, as expected, a marked rescue following treatment with elexacaftor/tezacaftor/ivacaftor, similar or even greater than that of F508del (Figure 3a). On the other side, R1066C, L1065P and L1065R displayed a negligible rescue upon treatment with lumacaftor, while the response to elexacaftor/tezacaftor/ivacaftor was slightly smaller than that of F508del.

We also analysed CFTR expression pattern in lysates of transfected CFBE41o-cells (Figure 3b). The results were in agreement with functional data. In agreement with previous findings (Seibert et al., 1996), the ICL4 variants are expressed as immature, core-glycosylated forms (Figure 3b). A significant appearance of band C was observed in cells treated with elexacaftor/tezacaftor (Figure 3b).

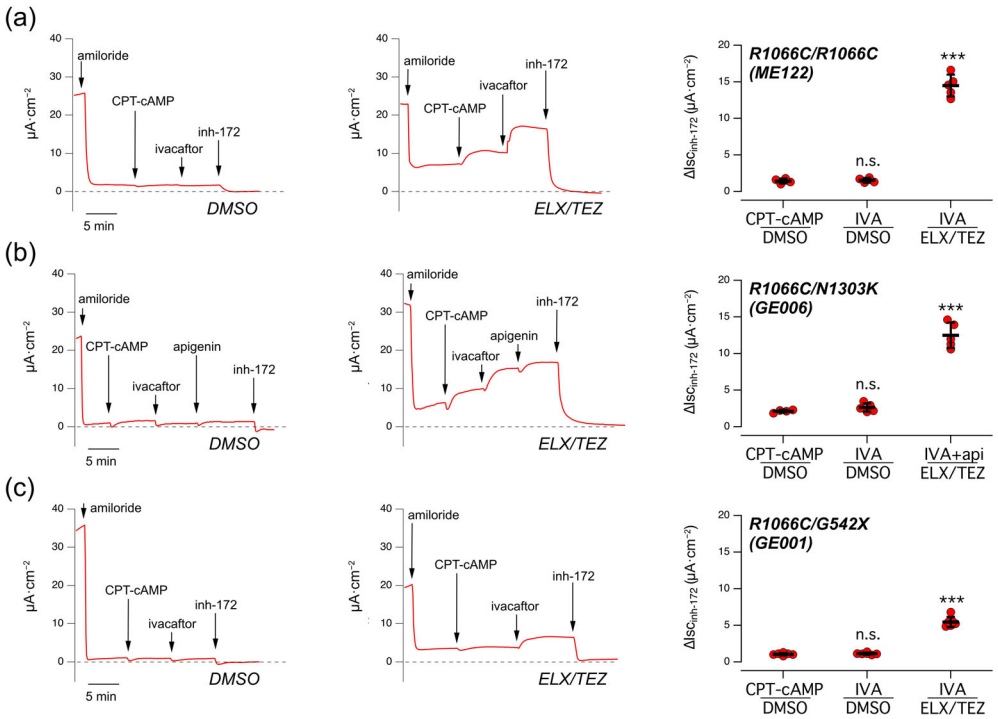

FIGURE 7 Functional evaluation of cystic fibrosis transmembrane conductance regulator (CFTR) activity and rescue by combined corrector treatment on nasal epithelia derived from people with CF (pwCF) bearing the R1066C variant. Epithelia were treated for 24 h with vehicle (DMSO), or elexacaftor (ELX)/ tezacaftor (TEZ) (3 μM/10 μM) prior to the assay. (a–c) Representative traces and scatter dot plots summarizing CFTR activity and the effect of drug treatments on R1066C/R1066C nasal epithelia (donor ID: ME122, n = 5; shown in [a]), R1066C/N1303K nasal epithelia (donor ID: GE006, n = 5; shown in [b]), R1066C/G542X nasal epithelia (donor ID: GE001, n = 6; shown in [c]), measured with the short-circuit current technique. Symbols indicate statistical significance of treatments: n.s., not significant; $^{***}P < 0.001$ versus DMSO/CPT-cAMP condition.

Interestingly, while chronic treatment with ivacaftor (in combination with elexacaftor/tezacaftor) caused a reduction in the band C amount for the F508del mutant, the mature form of rescued L1065P and L1065R appeared to be more resistant to the detrimental effect of the chronic potentiator treatment.

In transiently transfected HEK293 cells, a similar functional restoration could be observed for L1065R, L1065P and R1066C (Figure 4a). Cell surface measurements of CFTR performed using the HiBiT complementation assay confirmed partial restoration of CFTR surface expression, in the same range as observed with F508del (Figure 4b). These results are in concordance with the ones obtained in transfected CFBE41o-cells.

3.3 | ETI restores CFTR-mediated chloride secretion in primary human nasal epithelial cells derived from CF individuals carrying ICL4 variants

To validate the results obtained on heterologous expression systems, we evaluated the sensitivity of ICL4 variants to pharmacological agents in native cell models using well-established methodologies already adopted for other CF mutations (Capurro et al., 2021; Sondo et al., 2022; Terlizzi et al., 2023; Tomati et al., 2023). We tested correctors/potentiators on primary nasal epithelial cells collected from people with CF with the selected mutations. Whenever homozygous subjects were not available (given the low frequency of these variants) we prioritized the recruitment of people with CF bearing the variants of interest on one allele and having, on the second allele, a minimal function (MF) mutation, that is, displaying negligible CFTR function and lack of response to modulators, to make sure that the observed effects of *in vitro* treatment can be assigned to the variant under investigation.

Nasal epithelia derived from people with CF with selected ICL4 variants were differentiated on porous membranes under air–liquid interface condition for 16–18 days. Then, epithelia were treated for 24 h with different correctors. In particular, we tested tezacaftor (10 μM), lumacaftor (3 μM), elexacaftor (3 μM) and the tezacaftor/elexacaftor combination. After treatment, correctors were removed, and epithelia were mounted in Ussing chamber-like systems for the measurement of CFTR function by short-circuit current recordings. During the recordings the following protocol was performed: First, ENaC-dependent Na^+ absorption was blocked by amiloride (apical side, 10 μM), then the membrane-permeable cAMP analogue CPT-cAMP was applied (apical and basolateral, 100 μM) to induce CFTR phosphorylation, followed by ivacaftor (apical, 0.1 μM) to potentiate CFTR function. Finally, **$CFTR_{inh}$-172** (apical, 20 μM) was added to block CFTR. The drop in the value of the current due to addition of $CFTR_{inh}$-172 was used as an estimate of total CFTR activity.

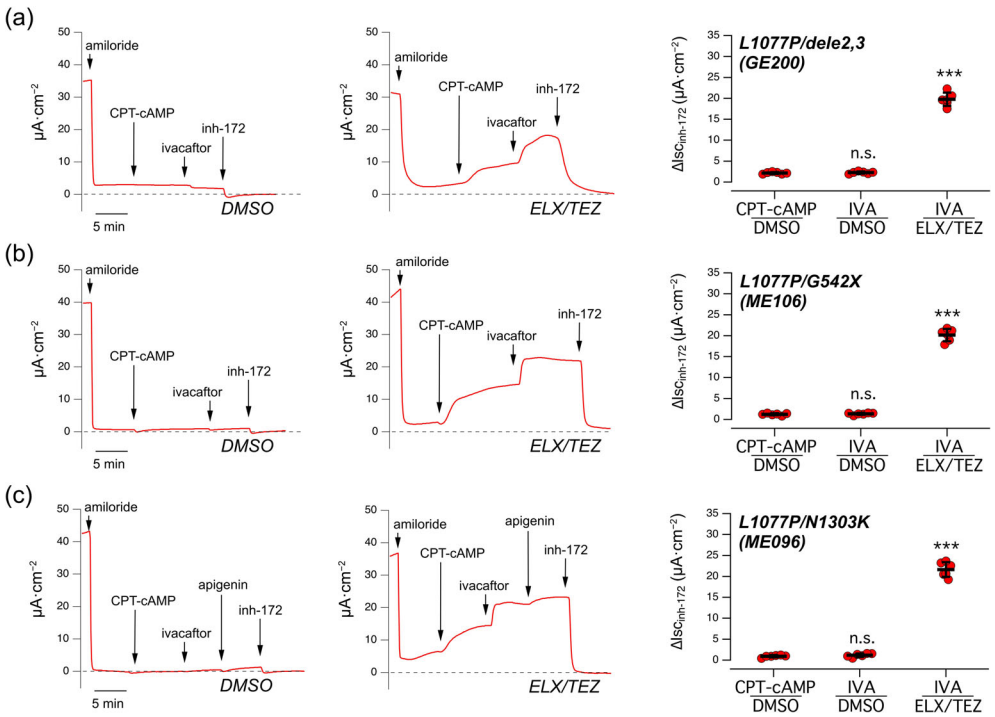

FIGURE 8 Functional evaluation of cystic fibrosis transmembrane conductance regulator (CFTR) activity and rescue by combined corrector treatment on nasal epithelia derived from people with CF (pwCF) bearing the L1077P variant. Epithelia were treated for 24 h with vehicle (DMSO), or elexacaftor (ELX)/ tezacaftor (TEZ) (3 μM/10 μM) prior to the assay. (a–c) Representative traces and scatter dot plots summarizing CFTR activity and the effect of drug treatments on L1077P/dele2,3 nasal epithelia (donor ID: GE200, n = 6; shown in [a]), L1077P/G542X nasal epithelia (donor ID: ME106, n = 6; shown in [b]), L1077P/N1303K nasal epithelia (donor ID: ME096, n = 6; shown in [c]), measured with the short-circuit current technique. Symbols indicate statistical significance of treatments: n.s., not significant; $^{***}P < 0.001$ versus DMSO/CPT-cAMP condition.

Under control conditions, that is, after treatment with vehicle (DMSO) alone, epithelia carrying the L1065P variant (in trans with a MF mutation) displayed nearly negligible CFTR function, with no effect upon acute ivacaftor addition (Figure 5). Treatment with a Type 1 corrector (lumacaftor or tezacaftor) rescued very poorly mutant CFTR activity, while a larger response to $CFTR_{inh}$-172 was observed with the Type 3 corrector elexacaftor (Figure 5). The elexacaftor/tezacaftor combination resulted to be the most effective treatment (Figure 5). CFTR-mediated current in elexacaftor/tezacaftor-treated epithelia, stimulated with the cAMP agonist and ivacaftor ranged around 11–13 μA. For comparison, the CFTR activity measured in epithelia derived from healthy donors ranges around 25–30 μA (Figure S1), while in elexacaftor/tezacaftor-treated epithelia from F508del/F508del people with CF, stimulated with the cAMP agonist and ivacaftor, the rescued CFTR activity ranged around 14–18 μA (Figure S2). Thus, the triple combination rescued up to 40% of total CFTR activity in L1065P/MF epithelia. When we tested elexacaftor/tezacaftor on epithelia derived from people with CF bearing L1065P in trans with another rescuable variant, the rescued CFTR activity increased up to 20 μA, corresponding to nearly 70% of the normal CFTR function (Figure 6). In case of epithelia bearing N1303K, we also added apigenin after ivacaftor to maximally stimulate channel activity (Figure 6).

Epithelia homozygous for the R1066C variant, treated with vehicle, displayed nearly absent CFTR-mediated activity (Figure 7a). In elexacaftor/tezacaftor-treated epithelia, stimulated with the cAMP agonist and ivacaftor, total CFTR activity increased up to 15 μA, corresponding to approximately 50% of the normal CFTR function (Figure 7a). A similar rescue was obtained on R1066C/N1303K epithelia, while on R1066C/MF epithelia CFTR-mediated current was

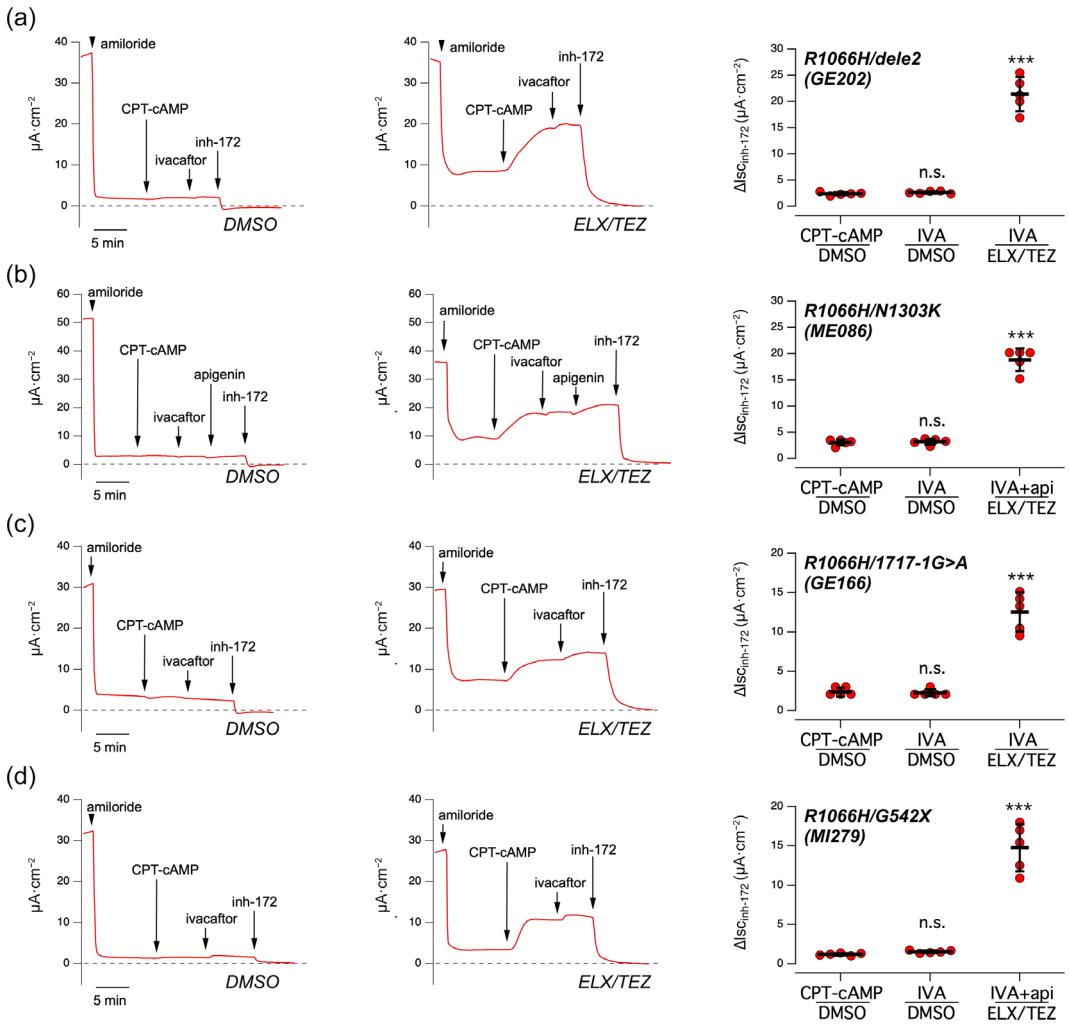

FIGURE 9 Functional evaluation of cystic fibrosis transmembrane conductance regulator (CFTR) activity and rescue by combined corrector treatment on nasal epithelia derived from people with CF bearing the R1066H variant. Epithelia were treated for 24 h with vehicle (DMSO), or elexacaftor (ELX)/ tezacaftor (TEZ) (3 μM/10 μM) prior to the assay. (a–d) Representative traces and scatter dot plots summarizing CFTR activity and the effect of drug treatments on L1077P/dele2,3 nasal epithelia (donor ID: GE202, n = 5; shown in [a]), R1066H/N1303K nasal epithelia (donor ID: ME086, n = 5–6; shown in [b]), R1066H1717-1G>A nasal epithelia (donor ID: GE166, n = 6; shown in [c]), R1066H/G542X nasal epithelia (donor ID: MI279, n = 6; shown in [d]), measured with the short-circuit current technique. Symbols indicate statistical significance of treatments: n.s., not significant; $^{***}P < 0.001$ versus DMSO/CPT-cAMP condition.

increased by the drug treatment up to approximately 6 μA (20% of the normal CFTR activity) (Figure 7b,c).

For comparison, we evaluated the effect of the triple combination on epithelia carrying two variants, L1077P and R1066H, considered by FDA eligible for this treatment (based on Fischer rat thyroid data). DMSO-treated epithelia carrying the L1077P mutation showed negligible CFTR activity, that increased up to 20–22 μA (corresponding to 65%–70% of normal CFTR current) in elexacaftor/tezacaftor-treated epithelia (Figure 8). Similar results were obtained on R1066H epithelia were tested, with a rescued CFTR activity ranging between 13–22 μA (around 45–70% of normal CFTR function) (Figure 9).

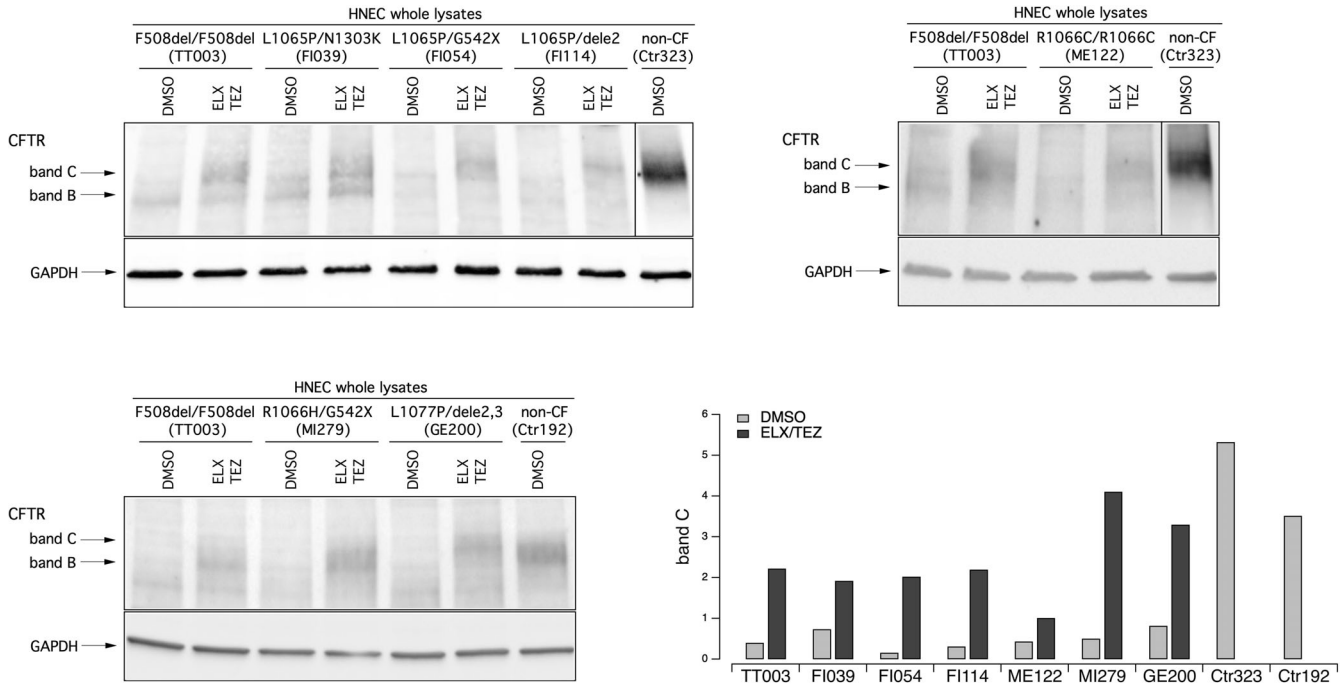

FIGURE 10 Biochemical analysis of cystic fibrosis transmembrane conductance regulator (CFTR) expression pattern and effect of CFTR-modulating drugs in patient-derived primary nasal epithelial cells carrying intracellular loop 4 (ICL4) variants. The representative western blot images show CFTR electrophoretic mobility in human nasal epithelial cell (HNEC) whole lysates following treatment for 24 h, prior to lysis, with the indicated modulators. Lysates from nasal epithelia derived from CF subjects homozygous for the F508del mutation, or from non-CF subjects are also shown for comparison. In the first two WBs, the line of separation indicates that, for Ctr323, an image acquired with a shorter exposure time is displayed. The bar graphs show CFTR band C densitometry of the western blot experiments. Due to the limited availability of patient-derived cells, this analysis was performed on a single lysate per condition for each donor, and only on selected subjects.

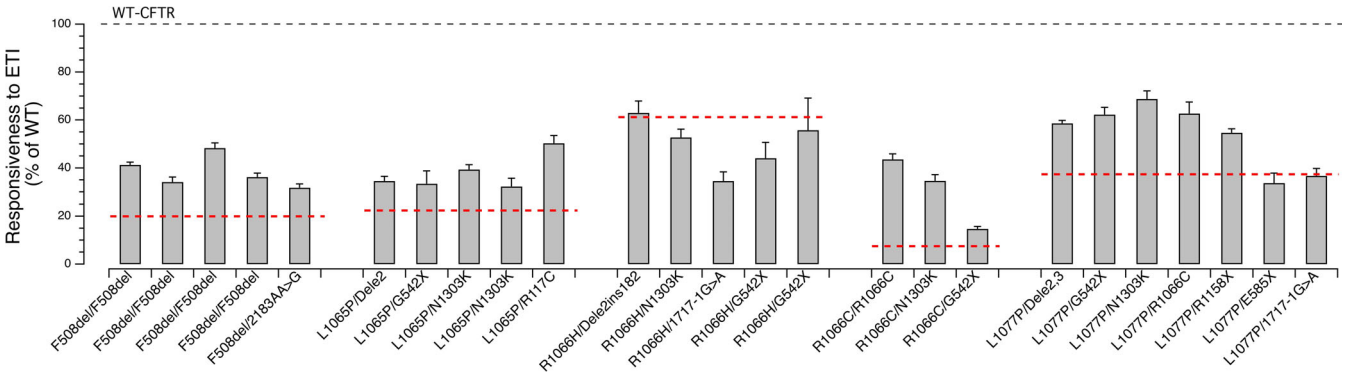

FIGURE 11 Comparison of the responsiveness to elexacaftor–tezacaftor–ivacaftor (ETI) measured on patient-derived nasal epithelia carrying F508del or variants localized in the ICL4 and on Fischer rat thyroid (FRT) cells expressing single variants. Each bar represents the net increment in cystic fibrosis transmembrane conductance regulator (CFTR) activity upon ETI treatment, expressed as % of non-WT, measured on nasal epithelia derived from a single CF donor (i.e. total CFTR function in ETI-treated epithelia–total CFTR function in DMSO-treated epithelia). The dashed lines show the mean response to ETI for (from the left to the right) F508del, L1065P, R1066H, R1066C and L1077P, as reported by Bihler and colleagues (Bihler et al., 2024).

For selected donors, CFTR expression pattern was evaluated on lysates of patient-derived nasal epithelia (Figure 10). The analysis showed that, under control condition (DMSO), CFTR ICL4 variants are expressed as immature protein band B. However, drug treatment caused the appearance of CFTR band C, corresponding to the mature, fully glycosylated form of CFTR. In agreement with functional data, the extent of rescue for L1065P and R1066C was similar (in the case of L1065P) or slightly smaller (in the case of R1066C) to that observed for the F508del variant or for ICL4 variants deemed eligible to ETI treatment (R1066H and L1077P; Figure 10).

We then compared ETI efficacy on patient-derived nasal epithelia with the values of rescued activity, expressed as percentage of WT-CFTR function, obtained for the different variants on Fischer rat thyroid cells, as recently reported by Bihler and colleagues (Bihler et al., 2024). The results are shown in Figure 11. For most of the variants we found a good correlation between responsiveness to ETI measured on native cells and on the heterologous expression system. For F508del, L1065P and L1077P the rescue observed on Fischer rat thyroid cells was slightly lower than that measured on nasal cells, while the rescue of the R1066H variants was greater on Fischer rat thyroid cells as compared to nasal cells. However, in the case of the R1066C variant, responsiveness to ETI was markedly underestimated on Fischer rat thyroid cells. Indeed, while on nasal epithelia the net increment following ETI ranged between 15% (in R1066C/MF epithelia) and 40% (in R1066C/R1066C epithelia) of WT-CFTR activity, on Fischer rat thyroid cells it fell well below the 10% cut-off value used to discriminate responsive variants (Bihler et al., 2024).

4 | DISCUSSION AND CONCLUSIONS

The CFTR2 database, updated on September 2024, includes a total of 1167 interpreted CFTR variants, however more than 2000 sequence variants are reported in the ClinVar database, the public archive of reports of human variations (Landrum et al., 2014; Landrum et al., 2020). Many of these variants still lack an in-depth characterization of the defect(s) displayed by the corresponding CFTR protein at the molecular and functional levels, nor it is known whether they are rescued by available modulators. However, given the very low frequency of most of the yet uncharacterized variants (being rare, ultra-rare or even private), the design and implementation of clinical trials (including the n-of-1 trials) to facilitate the extension of the label of modulators is not feasible and/or sustainable.

Given the scarcity or absence of clinical data to support the approval of available modulators for people with CF bearing variants still orphan of treatment, predictive models have been developed to establish responsiveness to modulators of specific CFTR mutants. The first model exploited the Fischer rat thyroid cell line as a heterologous expression system for the CFTR variants under investigation and led to the first approval by the FDA of ETI (elexacaftor–tezacaftor–ivacaftor) for 177 variants. It has to be noted that, while the responsive variants were disclosed and are also listed in the prescription label of the drugs (https://www.accessdata.fda.gov/drugsatfda_docs/label/2023/212273s011,217660s002lbl.pdf), no disclosure was made about the total number and identity of the tested variants, nor about possible non-responsive variants. In addition to this, the cut-off value for discriminating responsive versus non-responsive variants was (arbitrarily) set at 10% of wild-type CFTR activity (https://www.accessdata.fda.gov/drugsatfda_docs/label/2023/212273s011,217660s002lbl.pdf). Although several studies estimated that 10%–35% of normal CFTR function can result in a milder cystic fibrosis phenotype (Van Goor et al., 2009; Zhang et al., 2009), this threshold was extrapolated either from *in vivo* studies on CF patients correlating CFTR activity with disease severity or from in *ex vivo*/*in vitro* analysis of CFTR activity in CF vs non-CF primary airway cells. Thus, it can be questioned whether this value may be applicable to measurements performed on heterologous expression systems. In addition, a recent study by the Sermet's group reporting data collected during the French compassionate programme showed that the patients whose human nasal epithelial cells (HNECs) displayed a correction >5% of the wild-type level exhibited an improvement in FEV_1% pred of >10% (Dreano et al., 2023). The authors considered this 5% as a physiologically relevant threshold (Dreano et al., 2023), as previous studies showed that in a CF epithelium, the genetic correction of 5% of the cells was enough to normalize the ion transport (Goldman et al., 1995).

Recently, the first academic study was performed by the Mense's group at the Cystic Fibrosis Foundation Therapeutics Laboratory and evaluated the responsiveness of 655 CFTR variants, reported as known or putatively disease-causing in the CFTR2 database (Bihler et al., 2024). This study also exploited Fischer rat thyroid cells as heterologous expression system for CFTR variants and drug response was estimated based on an increment of at least 10% of normal CFTR activity upon treatment with modulators (Bihler et al., 2024). The authors identified 292 additional variants showing low-medium baseline activity (<50% of normal CFTR Cl^- transport activity) that was increased by >10% following drug treatment (Bihler et al., 2024). To be noted, the authors stressed that the threshold of 10% functional improvement relative to wild-type function should not be considered as a rigid cut-off (Bihler et al., 2024). Interestingly, the authors also reported that 5 of the 174 Trikafta approved variants that were included in their study clearly missed the ≥10% response threshold (G85E, R352W, S364P, L1324P and L1335P). Accordingly, a recent work from our group reported that, on patient-derived nasal epithelia, elexacaftor/tezacaftor rescued only partially the maturation defect of G85E-CFTR, with a rescued CFTR-mediated activity that reached 15%–25% of the activity measured in non-CF epithelia (Tomati et al., 2024). This value fell well below the rescue of F508del by elexacaftor/tezacaftor, ranging between 40% and 65% (Capurro et al., 2021; Veit et al., 2020). Consistently, a modest clinical benefit for three individuals taking ETI was observed, although the improvement was smaller than that of F508del heterozygotes treated with elexacaftor/tezacaftor (Middleton et al., 2019), in agreement with the *ex vivo*/*in vitro* data (Tomati et al., 2024). Clinical efficacy of ETI on people with CF carrying the G85E variant was also demonstrated by several real-word studies (Burgel et al., 2024; Dreano et al., 2023; Graeber et al., 2023).

Discrepancies on the responsiveness to modulators in different models have been observed for other variants. An example is R334W, which was found to be non-responsive to ETI on Fischer rat thyroid cells (Bihler et al., 2024), but whose rescue was demonstrated in patient-derived primary nasal epithelia (Dreano et al., 2023; Pion et al., 2024) and confirmed in clinical settings (Burgel et al., 2024; Dreano et al., 2023; Pion et al., 2024). So far, R334W is still an orphan mutation.

In the present study, we provide evidence that other two orphan mutations, L1065P and R1066C, can be rescued by ETI. Importantly, experiments on nasal epithelial cells from patients with such mutations revealed a substantial effect. The CFTR-mediated current was negligible in vehicle-treated cells but, after treatment with the triple combination reached 15%–20% (for R1066C) and 40%–45% (for L1065P) of the activity measured in non-CF epithelia. Although the observed rescue was smaller than that of the F508del (40–65% of the normal activity), it should fall in a range predicted to provide a clinical benefit (Dreano et al., 2023). Interestingly, our results are in line with those were recently reported by Conti and colleagues, who investigated L1065P and R1066H function and rescue in intestinal monolayers and organoids derived from two patients carrying these variants in combination with a MF variant (Conti et al., 2025). Analyses of the single variants expressed heterologously in immortalized bronchial cells further supported the efficacy of the triple combination at the protein and functional level with a rescue close to 50% of wild-type CFTR. Interestingly, the R1066C variant, analysed on Fischer rat thyroid cells, failed to reach the cut-off value for responding variants (Bihler et al., 2024) supporting the previous finding from our and other groups that cell background may affect mutant CFTR processing and activity (Berical et al., 2022; Cholon & Gentzsch, 2018; Cholon & Gentzsch, 2022; Pedemonte et al., 2010; Tomati et al., 2023).

These results are a strong indication for the treatment of patients carrying L1065P and R1066C with CFTR modulators since the results obtained in our study predict a significant clinical benefit. From the mechanistic point of view, our results further confirm that CFTR modulators have a global effect on CFTR protein structure with correcting effects on mutations localized in different domains of the protein.

From a more general point of view, this study also supports the predictive value of nasal cell models for personalized medicine approaches. Besides the possibility to characterize rare CFTR variants, the nasal epithelial cell model also allows to address the response to drugs exhibited by native CF cells that express combinations of two CFTR variants (Pion et al., 2024), a situation that is not possible to mimic in heterologous expression systems (like the Fischer rat thyroid cells). In addition, patient-derived nasal cells encompass the whole genetic background of the donors, possible unmasking the effects of modifiers that may influence CFTR variant expression, function and rescue by modulators. In this view, we have to consider that modifiers may be differentially expressed in cell models, thus explaining the discordant results obtained for the R1066C variants in Fischer rat thyroid cells as compared to primary cells. While the relevance of the Fischer rat thyroid cells as a model to assess drug responsiveness of CFTR variants is undeniable and meritoriously recognized by the regulatory authorities, patient-derived cell models have the potential to play a key role in the implementation of personalized approaches.

AUTHOR CONTRIBUTIONS

E. Pesce: Investigation (lead); methodology (lead). **V. Tomati:** Investigation (equal); methodology (lead). **Valeria Capurro:** Investigation (equal). **M. Lena:** Investigation (equal). **C. Pastorino:** Investigation (equal). **M. Astore:** Investigation (equal); methodology (lead). **S. Kuyucak:** Methodology (equal). **B. Chevalier:** Investigation (equal). **E. Sondo:** Investigation (equal); methodology (equal). **F. Cresta:** Investigation (equal); methodology (lead). **A. Dighero:** Investigation (equal). **V. Terlizzi:** Investigation (equal); methodology (equal). **C. Fevola:** Investigation (equal). **S. Costa:** Investigation (equal); methodology (equal). **M. C. Lucanto:** Investigation (equal); methodology (equal). **V. Daccò:** Investigation (equal); methodology (equal). **L. Claut:** Investigation (equal); methodology (equal). **F. Ficili:** Investigation (equal); methodology (equal). **B. Fabrizzi:** Investigation (equal); methodology (equal). **R. Bocciardi:** Data curation (equal); methodology (equal); resources (equal); writing—review and editing (equal). **F. Zara:** Funding acquisition (equal); resources (equal). **C. Castellani:** Data curation (equal); funding acquisition (equal); resources (equal); supervision (equal); writing—review and editing (equal). **L. J. V. Galietta:** Data curation (equal); resources (equal); supervision (equal); visualization (equal); writing—original draft (equal); writing—review and editing (equal). **S. A. Waters:** Data curation (equal); resources (equal); supervision (equal); visualization (equal); writing—review and editing (equal). **A. Hinzpeter:** Data curation (equal); resources (equal); supervision (equal); visualization (equal); writing—review and editing (equal). **N. Pedemonte:** Conceptualization (lead); data curation (equal); funding acquisition (lead); methodology (equal); resources (lead); supervision (equal); visualization (equal); writing—original draft (lead); writing—review and editing (equal).

AFFILIATIONS

[1]UOC Genetica Medica, IRCCS Istituto Giannina Gaslini, Genoa, Italy
[2]Department of Neurosciences, Rehabilitation, Ophthalmology, Genetics, Maternal and Child Health (DINOGMI), University of Genoa, Genoa, Italy
[3]School of Physics, The University of Sydney, Sydney, New South Wales, Australia
[4]INSERM, CNRS, Institut Necker Enfants Malades, Paris, France
[5]Université Paris-Cité, Paris, France
[6]UOSD Centro Fibrosi Cistica, IRCCS Istituto Giannina Gaslini, Genoa, Italy
[7]Department of Pediatric Medicine, Meyer Children's Hospital IRCCS, Cystic Fibrosis Regional Reference Center, Florence, Italy
[8]Centro Hub Fibrosi Cistica, Azienda Ospedaliera Universitaria Policlinico G. Martino, Messina, Italy
[9]Department of Pediatrics, Cystic Fibrosis Center, Fondazione IRCCS Ca' Granda, Ospedale Maggiore Policlinico, Milan, Italy
[10]Cystic Fibrosis Center, Ospedale Giovanni Di Cristina, Palermo, Italy
[11]Cystic Fibrosis Regional Centre, Unit of Emerging and Immunosuppressed Infectious Diseases, Department of

Gastroenterology and Transplantation, Azienda Ospedaliero-Universitaria 'Ospedali Riuniti', Ancona, Italy
[12]Telethon Institute of Genetics and Medicine (TIGEM), Pozzuoli, Italy
[13]School of Clinical Medicine, Discipline of Paediatrics and Child Health, Faculty of Medicine and Health, UNSW Sydney, Sydney, New South Wales, Australia
[14]Molecular and Integrative Cystic Fibrosis Research Centre, UNSW Sydney, Sydney, New South Wales, Australia
[15]School of Biomedical Sciences, Faculty of Medicine and Health, UNSW Sydney, Sydney, New South Wales, Australia
[16]Department of Respiratory Medicine, Sydney Children's Hospital, Sydney, New South Wales, Australia

ACKNOWLEDGEMENTS

We gratefully thank the people with CF for their participation to this study and their continuous support to our work.

CONFLICT OF INTEREST STATEMENT

The authors declare no competing interests.

DATA AVAILABILITY STATEMENT

The data that support the findings of this study are available from the corresponding author upon reasonable request. Some data may not be made available because of privacy or ethical restrictions.

DECLARATION OF TRANSPARENCY AND SCIENTIFIC RIGOUR

This Declaration acknowledges that this paper adheres to the principles for transparent reporting and scientific rigour of preclinical research as stated in the *BJP* guidelines for Design and Analysis, and Immunoblotting and Immunochemistry, and as recommended by funding agencies, publishers and other organizations engaged with supporting research.

ORCID

Luis J. V. Galietta https://orcid.org/0000-0001-8686-3461
Nicoletta Pedemonte https://orcid.org/0000-0002-5161-1720

REFERENCES

Alexander, S. P. H., Mathie, A. A., Peters, J. A., Veale, E. L., Striessnig, J., Kelly, E., Armstrong, J. F., Faccenda, E., Harding, S. D., Davies, J. A., Aldrich, R. W., Attali, B., Baggetta, A. M., Becirovic, E., Biel, M., Bill, R. M., Caceres, A. I., Catterall, W. A., Conner, A. C., … Zhu, M. (2023). The Concise Guide to PHARMACOLOGY 2023/24: Ion channels. *British Journal of Pharmacology*, *180*(Suppl 2), S145–S222. https://doi.org/10.1111/bph.16178

Alexander, S. P. H., Fabbro, D., Kelly, E., Mathie, A. A., Peters, J. A., Veale, E. L., Armstrong, J. F., Faccenda, E., Harding, S. D., Davies, J. A., Annett, S., Boison, D., Burns, K. E., Dessauer, C., Gertsch, J., Helsby, N. A., Izzo, A. A., Ostrom, R., Papapetropoulos, A., … Wong, S. S. (2023). The Concise Guide to PHARMACOLOGY 2023/24: Enzymes. *British Journal of Pharmacology*, *180*(Suppl 2), S289–S373. https://doi.org/10.1111/bph.16181

Alexander, S. P. H., Roberts, R. E., Broughton, B. R. S., Sobey, C. G., George, C. H., Stanford, S. C., Cirino, G., Docherty, J. R., Giembycz, M. A., Hoyer, D., Insel, P. A., Izzo, A. A., Ji, Y., MacEwan, D. J., Mangum, J., Wonnacott, S., & Ahluwalia, A. (2018). Goals and practicalities of immunoblotting and immunohistochemistry: A guide for submission to the *British Journal of Pharmacology*. *British Journal of Pharmacology*, *175*, 407–411. https://doi.org/10.1111/bph.14112

Allan, K. M., Astore, M. A., Fawcett, L. K., Wong, S. L., Chen, P. C., Griffith, R., Jaffe, A., Kuyucak, S., & Waters, S. A. (2022). S945L-CFTR molecular dynamics, functional characterization and tezacaftor/ivacaftor efficacy in vivo and in vitro in matched pediatric patient-derived cell models. *Frontiers in Pediatrics*, *10*, 1062766. https://doi.org/10.3389/fped.2022.1062766

Allan, K. M., Astore, M. A., Kardia, E., Wong, S. L., Fawcett, L. K., Bell, J. L., Visser, S., Chen, P. C., Griffith, R., Jaffe, A., Sivam, S., Vittorio, O., Kuyucak, S., & Waters, S. A. (2023). Q1291H-CFTR molecular dynamics simulations and ex vivo theratyping in nasal epithelial models and clinical response to elexacaftor/tezacaftor/ivacaftor in a Q1291H/F508del patient. *Frontiers in Molecular Biosciences*, *10*, 1148501. https://doi.org/10.3389/fmolb.2023.1148501

Bacalhau, M., Camargo, M., Magalhães-Ghiotto, G. A. V., Drumond, S., Castelletti, C. H. M., & Lopes-Pacheco, M. (2023). Elexacaftor-tezacaftor-ivacaftor: A life-changing triple combination of CFTR modulator drugs for cystic fibrosis. *Pharmaceuticals (Basel)*, *16*(3), 410. https://doi.org/10.3390/ph16030410

Bear, C., & Ratjen, F. (2023). Charting the path to expanded access for CFTR modulator drugs: The nose knows. *European Respiratory Journal*, *62*(4), 2301387. https://doi.org/10.1183/13993003.01387-2023

Beaudet, A. L. (1992). Genetic testing for cystic fibrosis. *Pediatric Clinics of North America*, *39*(2), 213–228. https://doi.org/10.1016/S0031-3955(16)38292-X

Berical, A., Lee, R. E., Lu, J., Beermann, M. L., le Suer, J. A., Mithal, A., Thomas, D., Ranallo, N., Peasley, M., Stuffer, A., Bukis, K., Seymour, R., Harrington, J., Coote, K., Valley, H., Hurley, K., McNally, P., Mostoslavsky, G., Mahoney, J., … Hawkins, F. J. (2022). A multimodal iPSC platform for cystic fibrosis drug testing. *Nature Communications*, *13*(1), 4270. https://doi.org/10.1038/s41467-022-31854-8

Berkers, G., van Mourik, P., Vonk, A. M., Kruisselbrink, E., Dekkers, J. F., de Winter-de Groot, K. M., Arets, H. G. M., Marck-van der Wilt, R. E. P., Dijkema, J. S., Vanderschuren, M. M., Houwen, R. H. J., Heijerman, H. G. M., van de Graaf, E. A., Elias, S. G., Majoor, C. J., Koppelman, G. H., Roukema, J., Bakker, M., Janssens, H. M., … van der Ent, C. K. (2019). Rectal organoids enable personalized treatment of cystic fibrosis. *Cell Reports*, *26*(7), 1701–1708. https://doi.org/10.1016/j.celrep.2019.01.068

Bihler, H., Sivachenko, A., Millen, L., Bhatt, P., Patel, A. T., Chin, J., Bailey, V., Musisi, I., LaPan, A., Allaire, N. E., Conte, J., Simon, N. R., Magaret, A. S., Raraigh, K. S., Cutting, G. R., Skach, W. R., Bridges, R. J., Thomas, P. J., & Mense, M. (2024). In vitro modulator responsiveness of 655 CFTR variants found in people with cystic fibrosis. *Journal of Cystic Fibrosis*, *23*(4), 664–675. https://doi.org/10.1016/j.jcf.2024.02.006

Brewington, J. J., Filbrandt, E. T., LaRosa, F. J. III, Moncivaiz, J. D., Ostmann, A. J., Strecker, L. M., & Clancy, J. P. (2018). Brushed nasal epithelial cells are a surrogate for bronchial epithelial CFTR studies. *JCI Insight*, *3*(13), e99385. https://doi.org/10.1172/jci.insight.99385

Burgel, P. R., Sermet-Gaudelus, I., Girodon, E., Durieu, I., Houdouin, V., Audousset, C., Macey, J., Grenet, D., Porzio, M., Murris-Espin, M., Reix, P., Baravalle, M., Belleguic, C., Mely, L., Verhille, J., Weiss, L., Reynaud-Gaubert, M., Mittaine, M., Hamidfar, R., … Nouvel, T. (2024). The expanded French compassionate programme for elexacaftor-tezacaftor-ivacaftor use in people with cystic fibrosis without a F508del CFTR variant: A real-world study. *Lancet Respiratory Medicine*, *12*(11), 888–900. https://doi.org/10.1016/S2213-2600(24)00208-X

Capurro, V., Tomati, V., Sondo, E., Renda, M., Borrelli, A., Pastorino, C., Guidone, D., Venturini, A., Giraudo, A., Mandrup Bertozzi, S.,

Musante, I., Bertozzi, F., Bandiera, T., Zara, F., Galietta, L. J. V., & Pedemonte, N. (2021). Partial Rescue of F508del-CFTR Stability and Trafficking Defects by Double Corrector Treatment. *International Journal of Molecular Sciences*, *22*(10), 5262. https://doi.org/10.3390/ijms22105262

Castaldo, G., Fuccio, A., Cazeneuve, C., Picci, L., Salvatore, D., Raia, V., Scarpa, M., Goossens, M., & Salvatore, F. (1999). Detection of five rare cystic fibrosis mutations peculiar to Southern Italy: Implications in screening for the disease and phenotype characterization for patients with homozygote mutations. *Clinical Chemistry*, *45*(7), 957–962. https://doi.org/10.1093/clinchem/45.7.957

Castellani, C., & Assael, B. M. (2017). Cystic fibrosis: A clinical view. *Cellular and Molecular Life Sciences*, *74*(1), 129–140. https://doi.org/10.1007/s00018-016-2393-9

Cholon, D. M., & Gentzsch, M. (2018). Recent progress in translational cystic fibrosis research using precision medicine strategies. *Journal of Cystic Fibrosis*, *17*(2), S52–S60. https://doi.org/10.1016/j.jcf.2017.09.005

Cholon, D. M., & Gentzsch, M. (2022). Established and novel human translational models to advance cystic fibrosis research, drug discovery, and optimize CFTR-targeting therapeutics. *Current Opinion in Pharmacology*, *64*, 102210. https://doi.org/10.1016/j.coph.2022.102210

Conti, J., Angyal, D., Kleinfelder, K., Latorre, R. V., Calicchia, M., Farinazzo, A., Rodella, L., Tomba, F., Massella, A., Frulloni, L., Taccetti, G., Terlizzi, V., Leung, A., Groeneweg, T. A., Bijvelds, M. J. C., Melotti, P., & Sorio, C. (2025). Evaluation of the response to elexacaftor-tezacaftor-ivacaftor of the rare CFTR variants L383S, I507del, L1065P and R1066H in intestinal organoid-derived epithelial monolayers. *Journal of Cystic Fibrosis*, *24*(3), 552–561. https://doi.org/10.1016/j.jcf.2025.02.008

Csanady, L., Vergani, P., & Gadsby, D. C. (2019). Structure, gating, and regulation of the CFTR anion channel. *Physiological Reviews*, *99*(1), 707–738. https://doi.org/10.1152/physrev.00007.2018

Curtis, M. J., Alexander, S. P. H., Cortese-Krott, M., Kendall, D. A., Martemyanov, K. A., Mauro, C., Panettieri, R. A. Jr., Papapetropoulos, A., Patel, H. H., Santo, E. E., Schulz, R., Stefanska, B., Stephens, G. J., Teixeira, M. M., Vergnolle, N., Wang, X., & Ferdinandy, P. (2025). Guidance on the planning and reporting of experimental design and analysis. *British Journal of Pharmacology*, *182*, 1413–1415. https://doi.org/10.1111/bph.17441

Cutting, G. R. (2015). Cystic fibrosis genetics: From molecular understanding to clinical application. *Nature Reviews. Genetics*, *16*(1), 45–56. https://doi.org/10.1038/nrg3849

De Boeck, K., & Amaral, M. D. (2016). Progress in therapies for cystic fibrosis. *The Lancet Respiratory Medicine*, *4*(8), 662–674. https://doi.org/10.1016/S2213-2600(16)00023-0

Dreano, E., Burgel, P. R., Hatton, A., Bouazza, N., Chevalier, B., Macey, J., Leroy, S., Durieu, I., Weiss, L., Grenet, D., Stremler, N., Ohlmann, C., Reix, P., Porzio, M., Roux Claude, P., Rémus, N., Douvry, B., Montcouquiol, S., Cosson, L., … French CF Reference Network study group. (2023). Theratyping cystic fibrosis patients to guide elexacaftor/tezacaftor/ivacaftor out-of-label prescription. *European Respiratory Journal*, *62*(4), 2300110. https://doi.org/10.1183/13993003.00110-2023

Estivill, X., Bancells, C., & Ramos, C. (1997). Geographic distribution and regional origin of 272 cystic fibrosis mutations in European populations. The Biomed CF Mutation Analysis Consortium. *Human Mutation*, *10*(2), 135–154. https://doi.org/10.1002/(SICI)1098-1004(1997)10:2<135::AID-HUMU6>3.0.CO;2-J

Feenstra, K. A., Hess, B., & Berendsen, H. J. C. (1999). Improving efficiency of large time-scale molecular dynamics simulations of hydrogen-rich systems. *Journal of Computational Chemistry*, *20*(8), 786–798. https://doi.org/10.1002/(SICI)1096-987X(199906)20:8<786::AID-JCC5>3.0.CO;2-B

Fiedorczuk, K., & Chen, J. (2022a). Mechanism of CFTR correction by type I folding correctors. *Cell*, *185*(1), 158–168 e11. https://doi.org/10.1016/j.cell.2021.12.009

Fiedorczuk, K., & Chen, J. (2022b). Molecular structures reveal synergistic rescue of Delta508 CFTR by Trikafta modulators. *Science*, *378*(6617), 284–290. https://doi.org/10.1126/science.ade2216

Galietta, L. J. V., Haggie, P. M., & Verkman, A. S. (2001). Green fluorescent protein-based halide indicators with improved chloride and iodide affinities. *FEBS Letters*, *499*(3), 220–224. https://doi.org/10.1016/S0014-5793(01)02561-3

Goldman, M. J., Yang, Y., & Wilson, J. M. (1995). Gene therapy in a xenograft model of cystic fibrosis lung corrects chloride transport more effectively than the sodium defect. *Nature Genetics*, *9*(2), 126–131. https://doi.org/10.1038/ng0295-126

Graeber, S. Y., Balázs, A., Ziegahn, N., Rubil, T., Vitzthum, C., Piehler, L., Drescher, M., Seidel, K., Rohrbach, A., Röhmel, J., Thee, S., Duerr, J., Mall, M. A., & Stahl, M. (2023). Personalized CFTR modulator therapy for G85E and N1303K homozygous patients with cystic fibrosis. *International Journal of Molecular Sciences*, *24*(15), 12365. https://doi.org/10.3390/ijms241512365

Horovitz, A., Matthews, J. M., & Fersht, A. R. (1992). Alpha-helix stability in proteins. II. Factors that influence stability at an internal position. *Journal of Molecular Biology*, *227*(2), 560–568. https://doi.org/10.1016/0022-2836(92)90907-2

Huang, J., Rauscher, S., Nawrocki, G., Ran, T., Feig, M., de Groot, B. L., Grubmüller, H., & MacKerell, A. D. Jr. (2017). CHARMM36m: An improved force field for folded and intrinsically disordered proteins. *Nature Methods*, *14*(1), 71–73. https://doi.org/10.1038/nmeth.4067

Landrum, M. J., Chitipiralla, S., Brown, G. R., Chen, C., Gu, B., Hart, J., Hoffman, D., Jang, W., Kaur, K., Liu, C., Lyoshin, V., Maddipatla, Z., Maiti, R., Mitchell, J., O'Leary, N., Riley, G. R., Shi, W., Zhou, G., Schneider, V., … Kattman, B. L. (2020). ClinVar: Improvements to accessing data. *Nucleic Acids Research*, *48*(D1), D835–D844. https://doi.org/10.1093/nar/gkz972

Landrum, M. J., Lee, J. M., Riley, G. R., Jang, W., Rubinstein, W. S., Church, D. M., & Maglott, D. R. (2014). ClinVar: Public archive of relationships among sequence variation and human phenotype. *Nucleic Acids Research*, *42*(Database issue), D980–D985. https://doi.org/10.1093/nar/gkt1113

Larsson, P., Kneiszl, R. C., & Marklund, E. G. (2020). MkVsites: A tool for creating GROMACS virtual sites parameters to increase performance in all-atom molecular dynamics simulations. *Journal of Computational Chemistry*, *41*(16), 1564–1569. https://doi.org/10.1002/jcc.26198

Lopes-Pacheco, M. (2019). CFTR modulators: The changing face of cystic fibrosis in the era of precision medicine. *Frontiers in Pharmacology*, *10*, 1662.

Meng, X., Clews, J., Ciuta, A. D., Martin, E. R., & Ford, R. C. (2019). CFTR structure, stability, function and regulation. *Biological Chemistry*, *400*(10), 1359–1370. https://doi.org/10.1515/hsz-2018-0470

Middleton, P. G., Mall, M. A., Dřevínek, P., Lands, L. C., McKone, E. F., Polineni, D., Ramsey, B. W., Taylor-Cousar, J. L., Tullis, E., Vermeulen, F., Marigowda, G., McKee, C. M., Moskowitz, S. M., Nair, N., Savage, J., Simard, C., Tian, S., Waltz, D., Xuan, F., … VX17-445-102 Study Group (2019). Elexacaftor-Tezacaftor-Ivacaftor for Cystic Fibrosis with a Single Phe508del Allele. *New England Journal of Medicine*, *381*(19), 1809–1819. https://doi.org/10.1056/NEJMoa1908639

Noel, S., Servel, N., Hatton, A., Golec, A., Rodrat, M., Ng, D. R. S., Li, H., Pranke, I., Hinzpeter, A., Edelman, A., Sheppard, D. N., & Sermet-Gaudelus, I. (2021). Correlating genotype with phenotype using CFTR-mediated whole-cell Cl(−) currents in human nasal epithelial cells. *Journal of Physiology*, *600*, 1515–1531. https://doi.org/10.1113/JP282143

Olesen, K., Awasthi, N., Bruhn, D. S., Pezeshkian, W., & Khandelia, H. (2018). Faster Simulations with a 5 fs Time Step for Lipids in the CHARMM Force Field. *Journal of Chemical Theory and Computation*, *14*(6), 3342–3350. https://doi.org/10.1021/acs.jctc.8b00267

Pedemonte, N. (2022). Nasal epithelial cells as a gold-standard predictive model for personalized medicine in cystic fibrosis. *The Journal of Physiology*, *600*, 1285–1286. https://doi.org/10.1113/JP282586

Pedemonte, N., Tomati, V., Sondo, E., & Galietta, L. J. V. (2010). Influence of cell background on pharmacological rescue of mutant CFTR. *American Journal of Physiology. Cell Physiology*, *298*(4), C866–C874. https://doi.org/10.1152/ajpcell.00404.2009

Pedemonte, N., Zegarra-Moran, O., & Galietta, L. J. (2011). High-throughput screening of libraries of compounds to identify CFTR modulators. *Methods in Molecular Biology*, *741*, 13–21. https://doi.org/10.1007/978-1-61779-117-8_2

Pion, A., Kavanagh, E., Joynt, A. T., Raraigh, K. S., Vanscoy, L., Langfelder-Schwind, E., McNamara, J., Moore, B., Patel, S., Merlo, K., Temme, R., Capurro, V., Pesce, E., Merlo, C., Pedemonte, N., Cutting, G. R., & Sharma, N. (2024). Investigation of CFTR Function in Human Nasal Epithelial Cells Informs Personalized Medicine. *American Journal of Respiratory Cell and Molecular Biology*, *71*(5), 577–588. https://doi.org/10.1165/rcmb.2023-0398OC

Sadras, I., Kerem, E., Livnat, G., Sarouk, I., Breuer, O., Reiter, J., Gileles-Hillel, A., Inbar, O., Cohen, M., Gamliel, A., Stanleigh, N., Gunawardena, T., Bartlett, C., Gonska, T., Moraes, T., Eckford, P. D. W., Bear, C. E., Ratjen, F., Kerem, B., … Cohen-Cymberknoh, M. (2023). Clinical and functional efficacy of elexacaftor/tezacaftor/ivacaftor in people with cystic fibrosis carrying the N1303K mutation. *Journal of Cystic Fibrosis*, *22*(6), 1062–1069. https://doi.org/10.1016/j.jcf.2023.06.001

Seibert, F. S., Linsdell, P., Loo, T. W., Hanrahan, J. W., Clarke, D. M., & Riordan, J. R. (1996). Disease-associated mutations in the fourth cytoplasmic loop of cystic fibrosis transmembrane conductance regulator compromise biosynthetic processing and chloride channel activity. *Journal of Biological Chemistry*, *271*(25), 15139–15145. https://doi.org/10.1074/jbc.271.25.15139

Sondo, E., Cresta, F., Pastorino, C., Tomati, V., Capurro, V., Pesce, E., Lena, M., Iacomino, M., Baffico, A. M., Coviello, D., Bandiera, T., Zara, F., Galietta, L. J. V., Bocciardi, R., Castellani, C., & Pedemonte, N. (2022). The L467F-F508del complex allele hampers pharmacological rescue of mutant CFTR by elexacaftor/tezacaftor/ivacaftor in cystic fibrosis patients: The value of the ex vivo nasal epithelial model to address non-responders to CFTR-modulating drugs. *International Journal of Molecular Sciences*, *23*(6), 3175. https://doi.org/10.3390/ijms23063175

Terlizzi, V., Pesce, E., Capurro, V., Tomati, V., Lena, M., Pastorino, C., Bocciardi, R., Zara, F., Centrone, C., Taccetti, G., Castellani, C., & Pedemonte, N. (2023). Clinical Consequences and Functional Impact of the Rare S737F CFTR Variant and Its Responsiveness to CFTR Modulators. *International Journal of Molecular Sciences*, *24*(7), 6576. https://doi.org/10.3390/ijms24076576

Tomati, V., Capurro, V., Pesce, E., Pastorino, C., Sondo, E., Lena, M., Borrelli, A., Cresta, F., Pantano, S., Collini, F., Ripani, P., Terlizzi, V., Fevola, C., Costa, S., Lucanto, M. C., Zara, F., Bandiera, T., Bocciardi, R., Castellani, C., … Pedemonte, N. (2024). Pharmacological rescue of the G85E CFTR variant by preclinical and approved modulators. *Frontiers in Pharmacology*, *15*, 1494327. https://doi.org/10.3389/fphar.2024.1494327

Tomati, V., Costa, S., Capurro, V., Pesce, E., Pastorino, C., Lena, M., Sondo, E., di Duca, M., Cresta, F., Cristadoro, S., Zara, F., Galietta, L. J. V., Bocciardi, R., Castellani, C., Lucanto, M. C., & Pedemonte, N. (2023). Rescue by elexacaftor-tezacaftor-ivacaftor of the G1244E cystic fibrosis mutation's stability and gating defects are dependent on cell background. *Journal of Cystic Fibrosis*, *22*(3), 525–537. https://doi.org/10.1016/j.jcf.2022.12.005

Van Der Spoel, D., Lindahl, E., Hess, B., Groenhof, G., Mark, A. E., & Berendsen, H. J. C. (2005). GROMACS: Fast, flexible, and free. *Journal of Computational Chemistry*, *26*(16), 1701–1718. https://doi.org/10.1002/jcc.20291

Van Goor, F., Hadida, S., Grootenhuis, P. D. J., Burton, B., Cao, D., Neuberger, T., Turnbull, A., Singh, A., Joubran, J., Hazlewood, A., Zhou, J., McCartney, J., Arumugam, V., Decker, C., Yang, J., Young, C., Olson, E. R., Wine, J. J., Frizzell, R. A., … Negulescu, P. (2009). Rescue of CF airway epithelial cell function in vitro by a CFTR potentiator, VX-770. *Proceedings of the National Academy of Sciences of the United States of America*, *106*(44), 18825–18830. https://doi.org/10.1073/pnas.0904709106

Van Goor, F., Hadida, S., Grootenhuis, P. D. J., Burton, B., Stack, J. H., Straley, K. S., Decker, C. J., Miller, M., McCartney, J., Olson, E. R., Wine, J. J., Frizzell, R. A., Ashlock, M., & Negulescu Paul, P. A. (2011). Correction of the F508del-CFTR protein processing defect in vitro by the investigational drug VX-809. *Proceedings of the National Academy of Sciences of the United States of America*, *108*(46), 18843–18848. https://doi.org/10.1073/pnas.1105787108

Veit, G., Avramescu, R. G., Chiang, A. N., Houck, S. A., Cai, Z., Peters, K. W., Hong, J. S., Pollard, H. B., Guggino, W. B., Balch, W. E., Skach, W. R., Cutting, G. R., Frizzell, R. A., Sheppard, D. N., Cyr, D. M., Sorscher, E. J., Brodsky, J. L., & Lukacs, G. L. (2016). From CFTR biology toward combinatorial pharmacotherapy: Expanded classification of cystic fibrosis mutations. *Molecular Biology of the Cell*, *27*(3), 424–433. https://doi.org/10.1091/mbc.e14-04-0935

Veit, G., Roldan, A., Hancock, M. A., da Fonte, D. F., Xu, H., Hussein, M., Frenkiel, S., Matouk, E., Velkov, T., & Lukacs, G. L. (2020). Allosteric folding correction of F508del and rare CFTR mutants by elexacaftor-tezacaftor-ivacaftor (Trikafta) combination. *JCI Insight*, *5*(18), e139983. https://doi.org/10.1172/jci.insight.139983

Wong, S. L., Awatade, N. T., Astore, M. A., Allan, K. M., Carnell, M. J., Slapetova, I., Chen, P. C., Capraro, A., Fawcett, L. K., Whan, R. M., Griffith, R., Ooi, C. Y., Kuyucak, S., Jaffe, A., & Waters, S. A. (2022). Molecular dynamics and functional characterization of I37R-CFTR lasso mutation provide insights into channel gating activity. *iScience*, *25*(1), 103710. https://doi.org/10.1016/j.isci.2021.103710

Zhang, L., Button, B., Gabriel, S. E., Burkett, S., Yan, Y., Skiadopoulos, M. H., Dang, Y. L., Vogel, L. N., McKay, T., Mengos, A., Boucher, R. C., Collins, P. L., & Pickles, R. J. (2009). CFTR delivery to 25% of surface epithelial cells restores normal rates of mucus transport to human cystic fibrosis airway epithelium. *PLoS Biology*, *7*(7), e1000155. https://doi.org/10.1371/journal.pbio.1000155

Zhang, Z., Liu, F., & Chen, J. (2018). Molecular structure of the ATP-bound, phosphorylated human CFTR. *Proceedings of the National Academy of Sciences of the United States of America*, *115*(50), 12757–12762. https://doi.org/10.1073/pnas.1815287115

SUPPORTING INFORMATION

Additional supporting information can be found online in the Supporting Information section at the end of this article.

How to cite this article: Pesce, E., Tomati, V., Capurro, V., Lena, M., Pastorino, C., Astore, M., Kuyucak, S., Chevalier, B., Sondo, E., Cresta, F., Dighero, A., Terlizzi, V., Fevola, C., Costa, S., Lucanto, M. C., Daccò, V., Claut, L., Ficili, F., Fabrizzi, B., … Pedemonte, N. (2025). *In silico*, *in vitro and ex vivo* characterization of cystic fibrosis transmembrane conductance regulator pathogenic variants localized in the fourth intracellular loop and their rescue by modulators. *British Journal of Pharmacology*, 1–18. https://doi.org/10.1111/bph.70176